Cyclic RGD Peptide-Conjugated Polyplex Micelles as a Targetable Gene Delivery System Directed to Cells Possessing $\alpha_v\beta_3$ and $\alpha_v\beta_5$ Integrins

Makoto Oba,[†] Shigeto Fukushima,[‡,§] Naoki Kanayama,[§,¶] Kazuhiro Aoyagi,[§] Nobuhiro Nishiyama,[#] Hiroyuki Koyama,[†] and Kazunori Kataoka*[,§,¶,#,⊥]

Department of Clinical Vascular Regeneration, Graduate School of Medicine, The University of Tokyo, 7-3-1 Hongo, Bunkyo, Tokyo 113-8655, Japan, R&D Division, Pharmaceuticals Group, Nippon Kayaku Co., Ltd., Department of Materials Engineering, Graduate School of Engineering, The University of Tokyo, 7-3-1 Hongo, Bunkyo, Tokyo 113-8656, Japan, CREST, Japan Science and Technology Agency, Japan, Center for Disease Biology and Integrative Medicine, Graduate School of Medicine, The University of Tokyo, 7-3-1 Hongo, Bunkyo, Tokyo 113-0033, Japan, and Center for NanoBio Integration, The University of Tokyo, 7-3-1 Hongo, Bunkyo, Tokyo 113-8656, Japan. Received January 15, 2007; Revised Manuscript Received May 11, 2007

A cyclic RGD peptide-conjugated block copolymer, cyclo[RGDfK(CX-)]−poly(ethylene glycol)−polylysine (c(RGDfK)−PEG−PLys), was synthesized from acetal-PEG−PLys under mild acidic conditions and spontaneously associated with plasmid DNA (pDNA) to form a polyplex micelle in aqueous solution. The cyclic RGD peptide recognizes $\alpha_v\beta_3$ and $\alpha_v\beta_5$ integrin receptors, which play a pivotal role in angiogenesis, vascular intima thickening, and the proliferation of malignant tumors. The c(RGDfK)−PEG−PLys/pDNA polyplex micelle showed a remarkably increased transfection efficiency (TE) compared to the PEG−PLys/pDNA polyplex micelle for the cultured HeLa cells possessing $\alpha_v\beta_3$ and $\alpha_v\beta_5$ integrins. On the other hand, in the transfection against the 293T cells possessing no $\alpha_v\beta_3$ and a few $\alpha_v\beta_5$ integrins, the TE of the c(RGDfK)−PEG−PLys/pDNA micelle showed no increase compared to the TE of the PEG−PLys/pDNA micelle. Flow cytometric analysis revealed a higher uptake of the c(RGDfK)−PEG−PLys/pDNA micelle than the PEG−PLys/pDNA micelle against HeLa cells, consistent with the transfection results. Furthermore, a confocal laser scanning microscopic observation revealed that the pDNA in the c(RGDfK)−PEG−PLys micelle preferentially accumulated in the perinuclear region of the HeLa cells within 3 h of incubation. No such fast and directed accumulation of pDNA to the perinuclear region was observed for the micelles without c(RGDfK) ligands. These results indicate that the increase in the TE induced by the introduction of the c(RGDfK) peptide ligand was due to an increase in cellular uptake as well as facilitated intracellular trafficking of micelles toward the perinuclear region via $\alpha_v\beta_3$ and $\alpha_v\beta_5$ integrin receptor-mediated endocytosis, suggesting that the cyclic RGD peptide-conjugated polyplex micelle has promising feasibility as a site-specifically targetable gene delivery system.

INTRODUCTION

With the increase in available information on various disease genes that has resulted from progress in the Human Genome Project, gene therapy is increasingly recognized as a promising therapy for many intractable diseases. Obviously, a major key to successful gene therapy is the development of gene vectors that are particularly effective for *in vivo* use. Nevertheless, there are many restrictions in the clinical application of viral vectors, which have played a pivotal role in gene therapy up to now, because of their safety issues, including antigenicity, as well as to the difficulty of formulating them with good quality control. These limitations of viral vectors have led to the recent trend in developing nonviral vectors with safety and high productivity as alternative systems to viral vectors.

One of the important challenges in the development of nonviral vectors is the system available for systemic injection, which must be stable enough to achieve longevity in the blood circulation but also be able to achieve high transfection efficiency (TE) in the target region with minimal toxicity. Lipoplex (*1*) and polyplex (*2*) systems based on cationic lipids and polymers, respectively, have been extensively studied as nonviral gene vectors for systemic administration. Nevertheless, there remain unresolved issues with these systems, because it is generally required that they contain excessive cationic lipids or polymers to increase solubility in an aqueous solution. Eventually, shifting their surface charge to a positive value induces nonspecific interaction with anionic components in the body such as plasma proteins and blood cells. This apparently hampers their applicability to systemic gene delivery. Polyplex micelles (*3*), characterized by the unique core−shell architecture of the hydrophilic shell layer surrounding their polyplex core, have the potential to acquire a so-called "stealth" property to minimize nonspecific interaction with biocomponents. Indeed, a polyplex micelle with poly(ethylene glycol) (PEG) as a hydrophilic shell layer achieved high stability in a medium containing serum compared to conventional lipoplexes and polyplexes and showed increased retention time in the bloodstream (*4*, *5*), suggesting that a polyplex micelle may be a promising candidate for a vector that can be used in systemic gene delivery. Nevertheless, in order to increase selective uptake into the target cells, appropriate ligands are preferably introduced into the surface of the polyplex micelles. In this way, surface-installed ligands are expected to enhance the uptake rate of the

* To whom correspondence should be addressed. Tel: +81-3-5841-7138, fax: +81-3-5841-7139, e-mail: kataoka@bmw.t.u-tokyo.ac.jp.
[†] Department of Clinical Vascular Regeneration, The University of Tokyo.
[‡] Nippon Kayaku Co., Ltd.
[§] Department of Materials Engineering, The University of Tokyo.
[¶] CREST.
[#] Graduate School of Medicine, The University of Tokyo.
[⊥] Center for NanoBio Integration, The University of Tokyo.

10.1021/bc0700133 CCC: $37.00
Published on Web 06/27/2007

polyplex micelles into the target cells by receptor-mediated endocytosis, which may lead to higher gene TE compared to the ligand-free polyplex micelles taken up by the cells through adsorptive or fluid-phase endocytosis (*6*−*8*).

In this study, acetal-poly(ethylene glycol)−polylysine (acetal-PEG−PLys) was synthesized as a precursor for constructing ligand-installed polyplex micelles. PLys, which is one of the first polymers used and well studied as a nonviral vector, was chosen as a cationic segment of the block copolymer. PLys-based polyplexes are known to show a relatively low TE against cultured cell lines compared to those having the endosomal escape function, such as polyethylenimine (PEI)-based polyplexes, but they have an advantage in stability even in a diluted condition, and they have shown an appreciable level of gene transfection in animal models (*5*, *9*). A cyclic RGD peptide (c(RGDfK)), which selectively recognizes $\alpha_v\beta_3$ and $\alpha_v\beta_5$ integrin receptors (*10*), was chosen as a ligand and introduced into the PEG terminus of aldehyde-PEG−PLys, derived from acetal-PEG−PLys, through a thiazolidine ring formation, and the c(RGDfK)−PEG−PLys block copolymer was obtained. It is generally known that the $\alpha_v\beta_3$ and $\alpha_v\beta_5$ integrins are expressed on various cell types such as endothelial cells, osteoclasts, macrophages, platelets, and melanomas, and that they play a significant role in angiogenesis, vascular intima thickening, and the proliferation of malignant tumors (*11*). Therefore, gene delivery targeting the $\alpha_v\beta_3$ and $\alpha_v\beta_5$ integrins is expected to be useful in the treatment of cancer and vascular diseases. Indeed, the c(RGDfK)−PEG−PLys/pDNA polyplex micelle thus prepared showed a remarkably increased TE compared to ligand-free polyplex micelles against the HeLa cells expressing $\alpha_v\beta_3$ and $\alpha_v\beta_5$ integrins.

EXPERIMENTAL PROCEDURES

Materials. 3,3-Diethoxypropanol was purchased from Aldrich Chemical Co. Ltd. (Milwaukee, WI). Ammonia solution (25%), tetrahydrofuran (THF), *N,N*-dimethylformamide (DMF), *n*-hexane, methanesulfonyl chloride (MsCl), and triethylamine (TEA) were purchased from Wako Pure Chem. Co. Ltd. (Japan). Ethylene oxide (EO) was purchased from Sumitomo Seika Chemicals Co. Ltd. (Japan). THF was distilled according to the conventional procedure as previously reported (*12*). DMF was dehydrated using activated molecular sieves (4A) and distilled under reduced pressure. 3,3-Diethoxypropanol and *n*-hexane were distilled over sodium wire. MsCl, TEA, and EO were dried over calcium hydride followed by distillation. CXYGGRGDS (RGDS) and cyclo[RGDfK(CX-)] (c(RGDfK)) peptides (X = 6-aminocaproic acid; ε-Acp) were purchased from Peptide Institute, Inc. (Japan). The PEG−PLys block copolymer (PEG; 12 000 g/mol, polymerization degree of PLys segment; 73) was synthesized as previously reported (*13*). A micro BCA protein assay reagent kit was purchased from Pierce (Rockford, IL). The Luciferase assay kit was a product of Promega (Madison, WI). Plasmid pCAcc+Luc coding for firefly luciferase under the control of the CAG promoter was provided by the RIKEN Gene Bank (Japan), amplified in competent DH5α *Escherichia coli*, and then purified using a HiSpeed Plasmid MaxiKit purchased from QIAGEN Sciences Co., Inc. (Germany). FITC-labeled monoclonal antibodies against $\alpha_v\beta_3$ integrin, $\alpha_v\beta_5$ integrin, and mouse IgG were purchased from Cosmo Bio Co., Ltd. (Japan). QuantiLum recombinant luciferase was purchased from Promega (Madison, WI).

Measurements. Gel permeation chromatography (GPC) measurements were carried out using a TOSOH HLC-8220 equipped with TSKgel columns (G4000PWXL and G3000PWXL). The internal refractive index (RI) was used for detection of the polymer. DMF with 10 mM LiCl was used as an eluent at a flow rate of 0.8 mL min^{-1} at 40 °C. IR was measured with an IR Report-100 spectrometer (JASCO, Tokyo, Japan). ^1H NMR spectra were obtained with a JEOL EX300 spectrometer (JEOL, Tokyo, Japan). Chemical shifts are reported in ppm relative to the residual protonated solvent resonance.

Synthesis of RGDS−PEG−PLys 5a and c(RGDfK)−PEG−PLys 5b (Scheme 1). *Acetal-PEG-NH_2 2.* A THF solution of 3,3-diethoxypropanol (0.16 mL, 1 mmol) and potassium naphthalene (2.7 mL, 0.90 mmol) were mixed in THF (75 mL) to form potassium 3,3-diethoxypropanolate (PDP) as previously reported (*14*). After the mixture was stirred for 10 min, liquid EO (13.5 mL, 270 mmol) chilled below 0 °C was added to the solution with additional stirring at room temperature (r.t.) for 2 days. The reactant polymer was isolated by precipitation into diethyl ether and lyophilized from benzene to obtain acetal-PEG-OH (12.65 g, quant). Acetal-PEG-OH (6.01 g, 0.50 mmol) was then dissolved in THF (40 mL), followed by the addition of TEA (0.32 mL, 2.25 mmol). Subsequently, the solution was slowly added dropwise into MsCl (0.12 mL, 1.5 mmol) in THF (20 mL) and stirred at 0 °C for 2 h. The solution was poured into diethyl ether to precipitate acetal-PEG-OMs **1**. The recovered acetal-PEG-OMs **1** was dissolved in 25% ammonia solution (500 mL) and stirred at r.t. for 4 days. The volume of the solution was concentrated to 50 mL by evaporation and dialyzed sequentially against 0.125% ammonia solution and distilled water, followed by lyophilization to obtain acetal-PEG-NH_2 **2** (5.40 g, 90%).

Acetal-PEG−PLys(TFA) 3. N^{ϵ}-Trifluoroacetyl-L-lysine *N*-carboxyanhydride (Lys(TFA)-NCA) (3.59 g, 13.39 mmol, 80 equiv to **2**) prepared according to the protocol described in the literature (*15*) in DMF (40 mL) was added to acetal-PEG-NH_2 **2** (2.01 g, 167.5 μmol) in DMF (20 mL) and stirred at 40 °C for 2 days. The polymerization was monitored by IR. The reactant polymer was precipitated into AcOEt/hexane (4:6) and lyophilized in dioxane to obtain acetal-PEG−PLys(TFA) **3** (4.08 g, 73%).

Acetal-PEG−PLys 4. NaOH solution (1 N, 4 mL) was added to acetal-PEG−PLys(TFA) **3** (500 mg, 17.77 μmol) in MeOH (40 mL) and stirred at 40 °C for 24 h. The reacted polymer was purified by dialysis sequentially against 10 mM PBS solution (pH 7.0) and distilled water and lyophilized to obtain acetal-PEG−PLys **4** (498 mg, quant).

*RGDS−PEG−PLys **6a** and c(RGDfK)−PEG−PLys **6b**.* Conjugation of the peptide into the PEG terminus of PEG−PLys was performed through thiazolidine ring formation using RGDS or c(RGDfK) peptide. RGDS−PEG−PLys **6a** was synthesized according to the typical procedure, as follows: Acetal-PEG−PLys **4** (39.1 mg, 1.64 μmol) was added to RGDS (15.2 mg, 16.4 μmol) in 0.2 M AcOH buffer (pH 4.0, 8 mL) and stirred at room temperature for 5 days. The reacted polymer was purified by dialysis sequentially against 10 mM PBS solution (pH 7.0) and distilled water and lyophilized to obtain RGDS−PEG−PLys **6a** (35.4 mg, 86%). Conjugation of the c(RGDfK) to acetal-PEG−PLys **4** was carried out in a similar way, e.g., c(RGDfK) (7.4 mg, 9.03 μmol) and acetal-PEG−PLys **4** (30.0 mg, 1.26 μmol) were used to obtain c(RGDfK)−PEG−PLys **6b** (26.6 mg, 87%).

Preparation of Polyplex Micelles. Each block copolymer and pDNA was dissolved separately in 10 mM Tris-HCl buffer (pH 7.4). The polymer solution in varying concentrations was added to a twice-excess volume of pDNA solution to form polyplex micelles with different compositions. The final pDNA concentration was adjusted to 33.3 or 50 μg/mL. The resulting solution was kept at r.t. overnight. The N/P ratio was defined as the residual molar ratio of the amino groups of PLys units to the phosphate groups of pDNA.

Ethidium Bromide Exclusion Assay. Polyplex micelle solutions (50 μg pDNA/mL) prepared at various N/P ratios were

Scheme 1. Syntheses of RGDS−PEG−PLys 6a and c(RGDfK)−PEG−PLys 6b

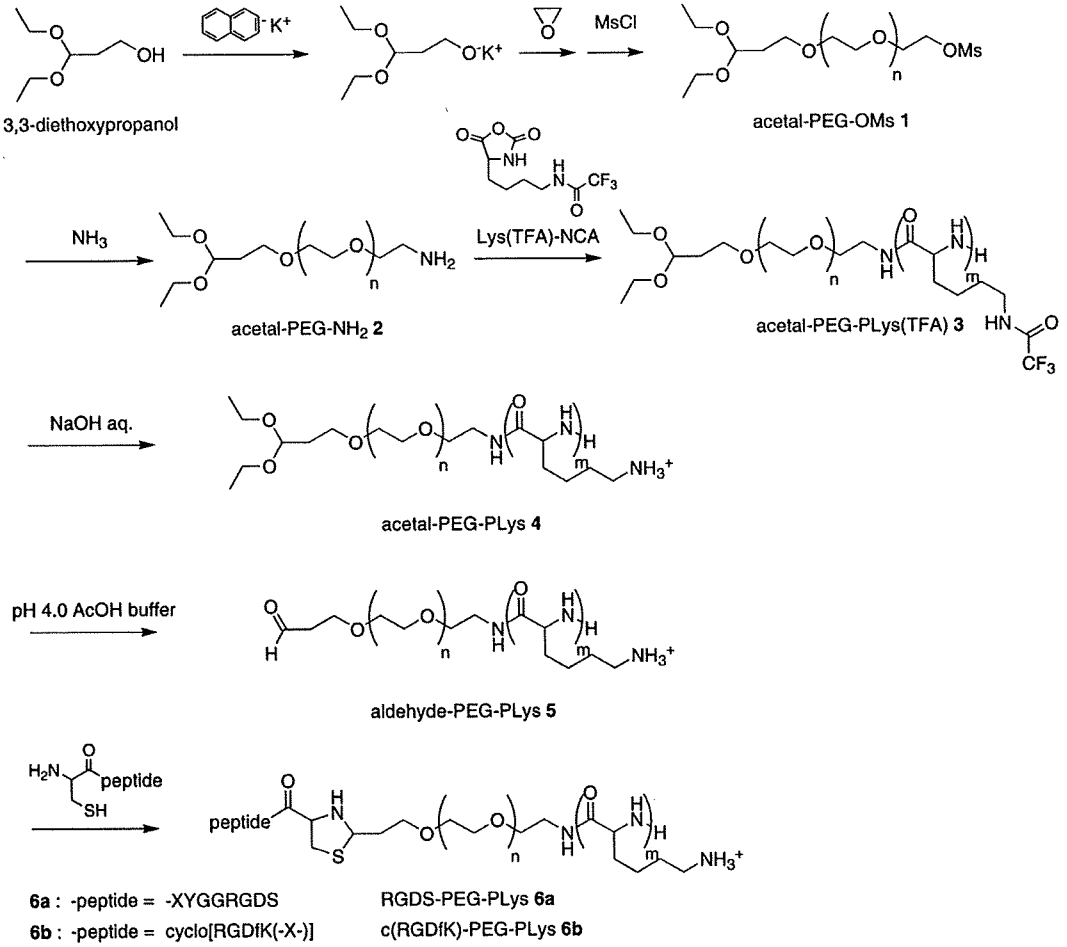

adjusted to contain 10 μg pDNA/mL with 2.5 μg ethidium bromide (EtBr)/mL and 150 mM NaCl by adding 10 mM Tris-HCl solution (pH 7.4) containing EtBr and NaCl. The solutions were kept at r.t. overnight. The fluorescence intensity of the sample solutions at 590 nm (excitation wavelength: 365 nm) was measured at 25 °C using a spectrofluorometer (ND-3300, NanoDrop, Wilmington, DE). The fluorescence intensity of naked pDNA was set at 100% and measured against a background of EtBr without pDNA.

Dynamic Light Scattering Measurement. The size of the polyplex micelles was evaluated by dynamic light scattering (DLS) using Nano ZS (ZEN3600, Malvern Instruments, Ltd., UK). A He−Ne ion laser (633 nm) was used as the incident beam. Polyplex micelle solutions (50 μg pDNA/mL) with an N/P = 2 were adjusted to a concentration of 10 μg pDNA/mL. The data obtained at a detection angle of 173 ° at 25 °C were analyzed by a cumulant method to obtain the hydrodynamic diameters and polydispersity indices (μ/Γ^2) of the micelles. The results reported are expressed as the mean values (±SEM) of three experiments.

ζ-Potential Measurement. The ζ-potential of polyplex micelles was evaluated by the laser-doppler electrophoresis method using Nano ZS with a He−Ne ion laser (633 nm). Sample solutions similar to those used for the DLS measurements were prepared. The ζ-potential measurements were carried out at 25 °C. A scattering angle of 17° was used in these measurements. The results are expressed as the mean values (±SEM) of three experiments.

Detection of $\alpha_v\beta_3$ and $\alpha_v\beta_5$ Integrin Receptors. 293T cells and HeLa cells were detached by pipetting and by harvesting with trypsin, respectively. Both types of cells were washed twice with PBS. The 1×10^6 cells and FITC-labeled antibody against $\alpha_v\beta_3$ or $\alpha_v\beta_5$ integrin (2 μg) were resuspended in 100 μL of Dulbecco's Modified Eagle Medium (DMEM) (containing 10% serum) and incubated on ice for 1 h in the dark. The cells were washed three times with cold medium and, after being resuspended in PBS, were analyzed using a flow cytometer (EPICS XL, Beckman Coulter, Inc.). The cytometric data were analyzed using EXPO32 software (Beckman Coulter, Inc., Fullerton, CA).

Transfection. HeLa and 293T cells were respectively seeded on 24-well culture plates (10 000 cells/well) and incubated overnight in 500 μL of DMEM containing 10% serum. After the medium was replaced with fresh medium, 20 μL of polyplex solution (50 μg pDNA/mL, N/P = 2) was applied to each well. The amount of pDNA was adjusted to 1 μg per well. After incubation for various lengths of time, the medium was replaced with 500 μL of fresh medium, followed by reincubation. The reincubation time was adjusted so the total incubation time would be 48 h. The luciferase gene expression was then evaluated based on the intensity of the photoluminescence using the Luciferase assay kit and a Luminometer (Lumat LB9507, BERTHOLD, Germany). The amount of protein in each well was concomitantly determined using a Micro BCA protein assay reagent kit. The relative light units were converted into the absolute amount of luciferase (ng) using a standard curve calibrated with recombinant luciferase (QuantiLum, Promega). One nanogram of luciferase corresponded to 9.1×10^7 RLU in our experiments; this was defined as the conversion factor.

Analysis of Cellular Uptake of Polyplex Micelles. pDNA was labeled with fluorescein as previously reported (*4*). Briefly,

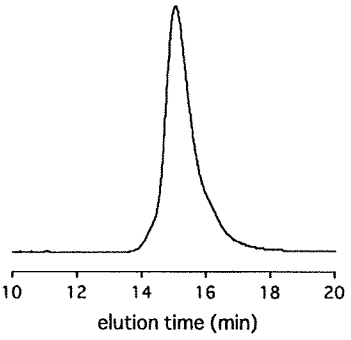

Figure 1. Gel permeation chromatogram of acetal-PEG−PLys(TFA) **3** (instrument TOSOH HLC-8220, detector RI, columns TSKgel G4000PWXL and G3000PWXL, eluent DMF with 10 mM LiCl, flow rate 0.8 mL min^{-1}, temperature 40 °C).

pDNA was labeled using a Label IT Nucleic Acid Labeling Kit (Mirus, Madison, WI). HeLa cells were seeded on six-well culture plates (100 000 cells/well) and incubated overnight in 1 mL of DMEM containing 10% serum. After the medium was replaced with fresh medium, 90 μL of polyplex solution (33.3 μg fluorescein-labeled pDNA/mL, N/P = 2) was applied to each well. The amount of fluorescein-labeled pDNA was adjusted to 3 μg per well. After various periods of incubation, the medium was removed and the cells were washed twice with PBS. After detachment by trypsin, the cells were resuspended in PBS and analyzed using the flow cytometer.

Confocal Laser Scanning Microscope (CLSM) Observation. pDNA was labeled with Cy5 in the same manner as fluorescein using the Label IT Nucleic Acid Labeling Kit. HeLa cells (30 000 cells) were seeded on a 35-mm glass base dish (Iwaki, Japan) and incubated overnight in 1 mL of DMEM containing 10% serum. After the medium was replaced with fresh medium, 90 μL of polyplex solution containing 3 μg Cy5-labeled pDNA (N/P = 2) was applied to a glass dish. After 3 h incubation, the medium was removed and the cells were washed twice with PBS. The intracellular distributions of the polyplex micelles were observed by CLSM following acidic late endosome and lysosome staining with LysoTracker Green (Molecular Probes, Eugene, OR) and nuclear staining with Hoechst 33342 (Dojindo Laboratories, Japan). The CLSM observation was performed using LSM 510 (Carl Zeiss, Germany) with a 63× objective (Ç-Apochromat, Carl Zeiss, Germany) at excitation wavelengths of 488 nm (Ar laser), 633 nm (He−Ne laser), and 710 nm (Mai Tai laser) for fluorescein, Cy5, and Hoechst 33342, respectively.

RESULTS

Synthesis of Peptide-Conjugated PEG−PLys (Scheme 1). The synthesis of acetal-PEG-OMs **1** has been previously reported (*14*). Briefly, PDP from 3,3-diethoxypropanol and potassium naphthalene initiated the anionic polymerization of EO to form acetal-PEG-OH (M_n 11 825, M_w 12 089, M_w/M_n 1.02), followed by the mesylation of alcohol using MsCl to obtain acetal-PEG-OMs **1**. Acetal-PEG-NH_2 **2** was then synthesized by amination of acetal-PEG-OMs **1** using ammonia solution and was confirmed to be unimodal with a narrow molecular weight distribution (M_w/M_n 1.03). Polymerization of Lys(TFA)-NCA using acetal-PEG-NH_2 **2** as an initiator led to the formation of acetal-PEG−PLys(TFA) **3**. A GPC of the obtained acetal-PEG−PLys(TFA) **3** showed a single peak with a narrow molecular weight distribution (M_w/M_n 1.12) (Figure 1). From the peak intensity ratio of the methylene protons of PEG (OCH_2CH_2, δ = 3.6 ppm) and the methylene protons of Lys(TFA) ($CH_2CH_2CH_2CH_2NH$, δ = 1.4, 1.5, 1.9, and 3.2 ppm) measured by ^{1}H NMR, the polymerization degree (DP) of Lys-

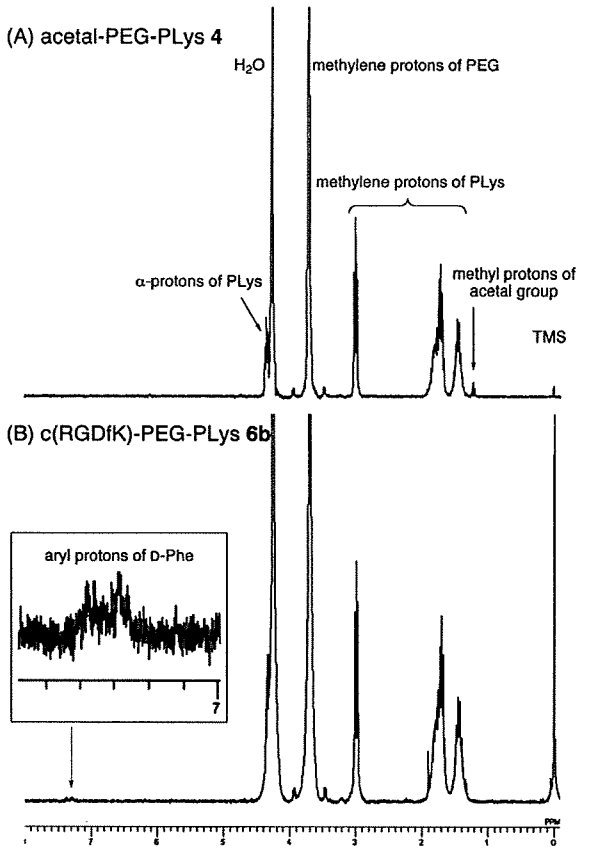

Figure 2. ^{1}H NMR spectra of acetal-PEG−PLys 4 (A) and c(RGDfK)−PEG−PLys **6b** (B) in D_2O at 80 °C.

(TFA) was calculated to be 70 (data not shown). Acetal-PEG−PLys **4** was then quantitatively obtained by the deprotection of acetal-PEG−PLys(TFA) **3** under basic conditions. From the ^{1}H NMR spectrum, the acetal group (CH_3CH_2O, δ = 1.2 ppm) was confirmed to be almost intact without converting to an aldehyde group (Figure 2). The DP of Lys was calculated to be 72 from the peak intensity ratio of the methylene protons of PEG (OCH_2CH_2, δ = 3.6 ppm) and the methylene protons of PLys ($CH_2CH_2CH_2CH_2NH_3$, δ = 1.4, 1.7, and 3.0 ppm) (Figure 2). The DP of acetal-PEG−PLys(TFA) **3** and acetal-PEG−PLys **4** were almost identical, indicating that main chain cleavage under the deprotection reaction was negligible.

Conjugation of peptide ligands into the PEG terminus of acetal-PEG−PLys **4** was achieved through the formation of a thiazolidine ring. The acetal group was deprotected under acidic conditions to an aldehyde group, giving aldehyde-PEG−PLys **5**. The aldehyde group is known to react with cysteine to form a stable thiazolidine ring (*16*). In this study, CXYGGRGDS (RGDS) and cyclo[RGDfK(CX-)] (c(RGDfK)), having an N-terminal cysteine residue (C: L-Cys), were reacted with acetal-PEG−PLys **4** under mild acidic conditions (pH 4.0) to prepare the peptide-conjugated PEG−PLys through thiazolidine formation. Note that Schiff base formation due to the reaction of the aldehyde and primary amino groups of the PLys segment was prohibited under the acidic conditions because of the complete protonation of the primary amino groups. The methyl protons of the acetal group (δ = 1.2 ppm) completely disappeared with the appearance of protons assigned to the aromatic rings of L-tyrosine (Y: L-Tyr:) (δ = 6.9 and 7.1 ppm) in the RGDS and D-phenylalanine (f: D-Phe) (δ = 7.3 and 7.4 ppm) in the c(RGDfK) (Figure 2). Based on the peak intensity ratios of the aromatic ring protons of peptide ligands and the methylene

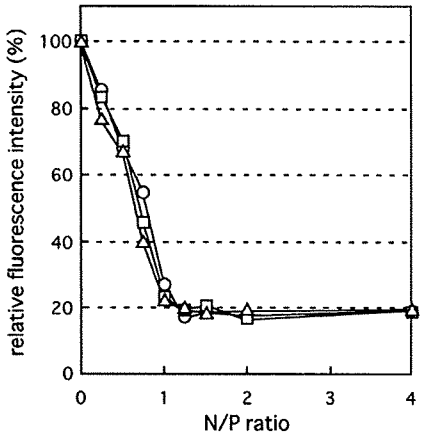

Figure 3. Ethidium bromide exclusion assays of PEG−PLys (open circle), RGDS−PEG−PLys (open square), and c(RGDfK)−PEG−PLys (open triangle). Fluorescence measurements were carried out as described in the Experimental Procedures.

Table 1. Size and ζ-Potentials of Polyplex Micelles

sample	cumulant diameter (nm)/ polydispersity index (μ/Γ^2)	ζ-potential (mV)
PEG−PLys	124 ± 0.27/0.158 ± 0.014	−0.19 ± 0.195
RGDS−PEG−PLys	124 ± 0.88/0.177 ± 0.012	1.12 ± 0.349
c(RGDfK)−PEG−PLys	125 ± 1.00/0.166 ± 0.006	0.68 ± 0.238

protons of PEG (OCH_2CH_2, δ = 3.6 ppm), the introduction rates of peptide ligands were determined to be 100% in the RGDS−PEG−PLys **6a** and 66% in the c(RGDfK)−PEG−PLys **6b**.

Formation of Polyplex Micelles. Ethidium bromide (EtBr) is known to form an intercalating complex with double helical polynucleotides and subsequently show a striking enhancement of its fluorescence intensity (*17*). This enhancement is quenched by the formation of a complex between DNA and cationic components, because cationic components prevent EtBr from intercalating into the double-strand DNA. Thus, EtBr exclusion assay is frequently utilized to estimate the degree of pDNA condensation in the complex with a catiomer (*18*, *19*). As shown in Figure 3, as the N/P ratio increased, the fluorescence intensity in all the polyplex micelles decreased correspondingly and leveled off at around N/P = 1.25. This result indicates that the degree of pDNA condensation was not influenced by the introduction of peptide ligands. Table 1 summarizes the cumulant diameters and ζ-potentials of the polyplex micelles at N/P = 2. The cumulant diameters of all the micelles were approximately 125 nm with a moderate polydispersity index between 0.15 and 0.18. There was no change in the particle size because of the introduction of peptide ligands. Also, the ζ-potentials of all the polyplex micelles were approximately 0 mV. As previously reported (*5*, *18*), the PEG palisade surrounding the complex shields the charge of the micelles to maintain a very small absolute value in the ζ-potential even in the region of N/P > 1. All of the results of the EtBr assay, DLS analysis, and ζ-potential measurement suggest that the characteristics of the three types of polyplex micelles (PEG−PLys, RGDS−PEG−PLys, and c(RGDfK)−PEG−PLys) were quite similar regardless of the introduction of the peptide ligands.

Detection of $\alpha_v\beta_3$ and $\alpha_v\beta_5$ Integrin Receptors. To evaluate the expression of integrin receptors on the cell surface, flow cytometric analysis of 293T and HeLa cells was carried out using FITC-labeled antibodies (Figure 4). Flow cytometric analysis revealed that the 293T cells expressed almost no $\alpha_v\beta_3$ integrin and a slight amount of $\alpha_v\beta_5$ integrin, while the HeLa cells expressed a considerably higher amount of $\alpha_v\beta_3$ and $\alpha_v\beta_5$ integrins than the 293T cells. These results implied that HeLa cells might show a higher uptake of the cyclic RGD peptide-conjugated polyplex micelles than 293T cells through integrin-mediated endocytosis.

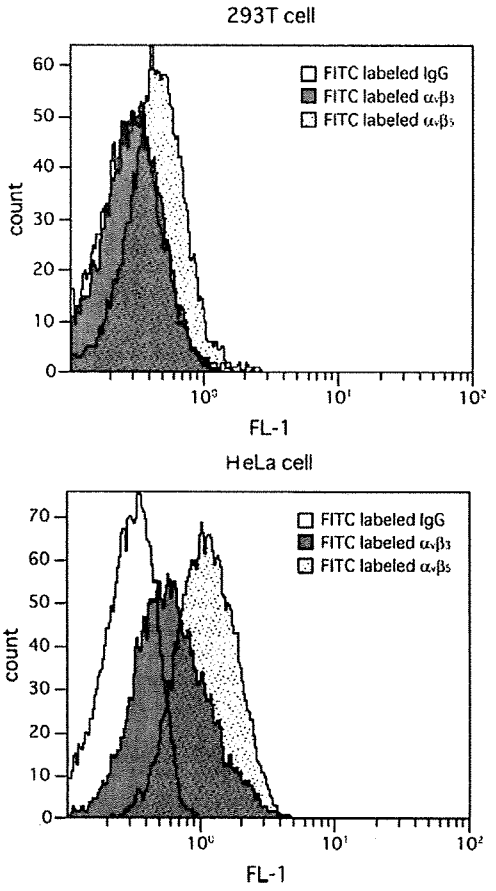

Figure 4. Flow cytometric analysis of integrin expression on 293T cells (left) and HeLa cells (right).

Transfection. *In vitro* TE of polyplex micelles was evaluated for 293T cells and HeLa cells at varying transfection times (Figure 5). PEG−PLys/pDNA micelles without the peptide ligand and RGDS−PEG−PLys/pDNA micelles with a linear RGD peptide ligand were used as controls. RGD peptide is the adhesion motif of extracellular matrix proteins for the various types of integrins (*20*, *21*). The linear RGD peptide showed a binding affinity for $\alpha_v\beta_3$ integrin approximately 1/1000 of that of the cyclic RGD peptide (*22*). In the transfection experiment using 293T cells, there were no differences in the TE of the three types of micelles at any of the transfection times. This finding is consistent with the observation that 293T cells showed low integrin expression (Figure 4). On the other hand, in the transfection experiment using HeLa cells, c(RGDfK)−PEG−PLys micelles achieved a significantly higher TE than PEG−PLys and RGDS−PEG−PLys micelles. It is reasonable to assume that HeLa cells might efficiently recognize c(RGDfK) ligands on the micelle through $\alpha_v\beta_3$ and $\alpha_v\beta_5$ integrins expressed on their surface. Nevertheless, the TE of linear RGD peptide-conjugated micelles toward HeLa cells was comparable to that of the micelles without any ligand, suggesting that the binding affinity of the linear RGD peptide for the integrins might be insufficient to increase the TE.

Analysis of Cellular Uptake of Polyplex Micelles. The cellular uptake of the micelles into the HeLa cells was evaluated by a flow cytometer using fluorescein-labeled pDNA-incorporated micelles with varying incubation times (Figure 6). The amount of the uptake was always higher for c(RGDfK)−PEG−

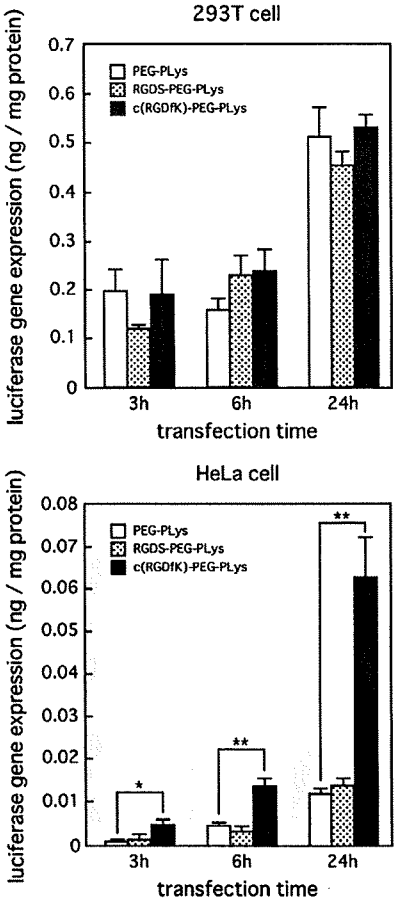

Figure 5. Effect of cell lines and transfection time on gene expression. 293T cells (left) and HeLa cells (right) were transfected with PEG–PLys, RGDS–PEG–PLys, and c(RGDfK)–PEG–PLys micelles prepared at N/P = 2 in a medium containing 10% serum. The data are the mean ± SEM, $n = 4$. $P^* < 0.05$ and $P^{**} < 0.01$.

PLys micelles than for PEG–PLys micelles at each incubation time, which suggests that the specific interaction of the cyclic RGD peptide with integrin receptors on the HeLa cells contributed to the uptake amount. In 24 h incubation, the amount of c(RGDfK)–PEG–PLys micelles that were taken up was 1.6 times the amount of PEG–PLys micelles taken up (Figure 6B). Nevertheless, c(RGDfK)–PEG–PLys micelles revealed an even higher TE of approximately 5 times that of the PEG–PLys micelles (Figure 5). This implied that other factors besides the enhanced uptake might also play a role in the enhanced TE observed for HeLa cells challenged with c(RGDfK)–PEG–PLys micelles.

Intracellular Distribution of Polyplex Micelles. The intracellular distribution of polyplex micelles was investigated by CLSM using Cy5-labeled pDNA-incorporated micelles with 3 h incubation, and typical images from this investigation are shown in Figure 7. A large fraction of the Cy5-labeled pDNA was still distributed near the cell membrane for the cells challenged with PEG–PLys polyplex micelles (Figure 7A). Alternatively, an appreciable accumulation of the Cy5-labeled pDNA in the perinuclear regions was observed for the cells challenged with c(RGDfK)–PEG–PLys polyplex micelles (Figure 7B). Further detailed observation using LysoTracker, which labels acidic late endosome and lysosome, revealed that the majority of c(RGDfK)–PEG–PLys polyplex micelles were localized in the acidic compartments as indicated by the yellow color in the merged fluorescence image of the Cy5-labeled pDNA (red) and LysoTracker (green), yet a fraction that did not co-localize with LysoTracker was also observed, suggesting that at least some of the polyplex micelles in the perinuclear regions may be located in a site other than the lysosomes.

DISCUSSION

There are many barriers to achieve effective transfection using nonviral gene vectors. Stability in the bloodstream and specific cellular uptake by the target tissues and organs are major obstacles, especially for *in vivo* gene delivery. Polyplex micelles with PEG as a hydrophilic shell layer have been shown to achieve an increased retention time in the bloodstream (*5*), and they are promising candidates for vectors that can be used for *in vivo* gene delivery. Also, the introduction of targetable ligands onto polyplex micelles has been reported, and some of the ligand-installed polyplex micelles have been demonstrated to be effective both in *in vivo* as well as *in vitro* transfection (*6*–*8*). The ligands on polyplex micelles may facilitate their internalization into the target cells, thus increasing the TE. A number of studies have aimed to find suitable ligands for this purpose (*23*), and cyclic RGD peptides have been highlighted as one of the promising candidates (*7*). Cyclic RGD peptides are well-known to selectively recognize $\alpha_v\beta_3$ and $\alpha_v\beta_5$ integrins, which are overexpressed in angiogenic endothelial cells in tumors. Therefore, a targetable gene delivery system equipped with a cyclic RGD peptide as the ligand may be useful for antiangiogenic therapy for tumors (*24*, *25*).

In this study, to construct polyplex micelles showing integrin-mediated gene transfection, the novel synthetic route of a block copolymer with a c(RGDfK) peptide ligand was exploited as summarized in Scheme 1. The acetal group may be converted to an aldehyde group under acidic conditions. Thus, the TFA group was selected to protect the primary amino group of the lysine units, because it can be removed under basic conditions without any conversion of acetal groups to aldehyde groups. The introduction of peptide ligands was then carried out under mild acidic conditions with good yields in a one-pot reaction involving the conversion of acetal groups to aldehyde groups and the subsequent conjugation of the ligand through the formation of a thiazolidine ring as seen in Scheme 1. In this way, various peptide ligands having a cysteine end group (Cys-peptide) may be readily introduced into the block copolymer. Moreover, this type of conjugation reaction between aldehyde and Cys-peptide occurs selectively even in the presence of primary amines, because the formation of a Schiff base between a primary amine and an aldehyde is reversible and thus sensitive to pH, while the thiazolidine ring formation between the N-terminal cysteine and aldehyde is an irreversible reaction. This reaction is available for the introduction of various ligands into the block copolymer, not only peptides but also other ligand molecules possessing an N-terminal cysteine.

Indeed, as confirmed by the NMR spectra shown in Figure 2, the c(RGDfK) peptide, which can peculiarly recognize $\alpha_v\beta_3$ and $\alpha_v\beta_5$ integrins, was successfully introduced into the PEG terminus of the PEG–PLys block copolymer as a targetable ligand molecule. The c(RGDfK)–PEG–PLys/pDNA micelle achieved a higher TE compared to nontargetable PEG–PLys and RGDS–PEG–PLys micelles against HeLa cells, which express an appreciable amount of $\alpha_v\beta_3$ and $\alpha_v\beta_5$ integrins. In contrast, there was no difference in TE among these three types of polyplex micelles against 293T cells, which show a limited expression of $\alpha_v\beta_5$ integrin, but no expression of $\alpha_v\beta_3$ integrin. This result is consistent with a previous report which found that the $\alpha_v\beta_3$ integrin has an approximately 10-times higher binding affinity for the cyclic RGD peptide than the $\alpha_v\beta_5$ integrin (*26*), which suggests that the $\alpha_v\beta_3$ integrin may be involved in an increased TE against HeLa cells by means of the c(RGDfK)–PEG–PLys/pDNA micelle. Flow cytometric analysis (Figure

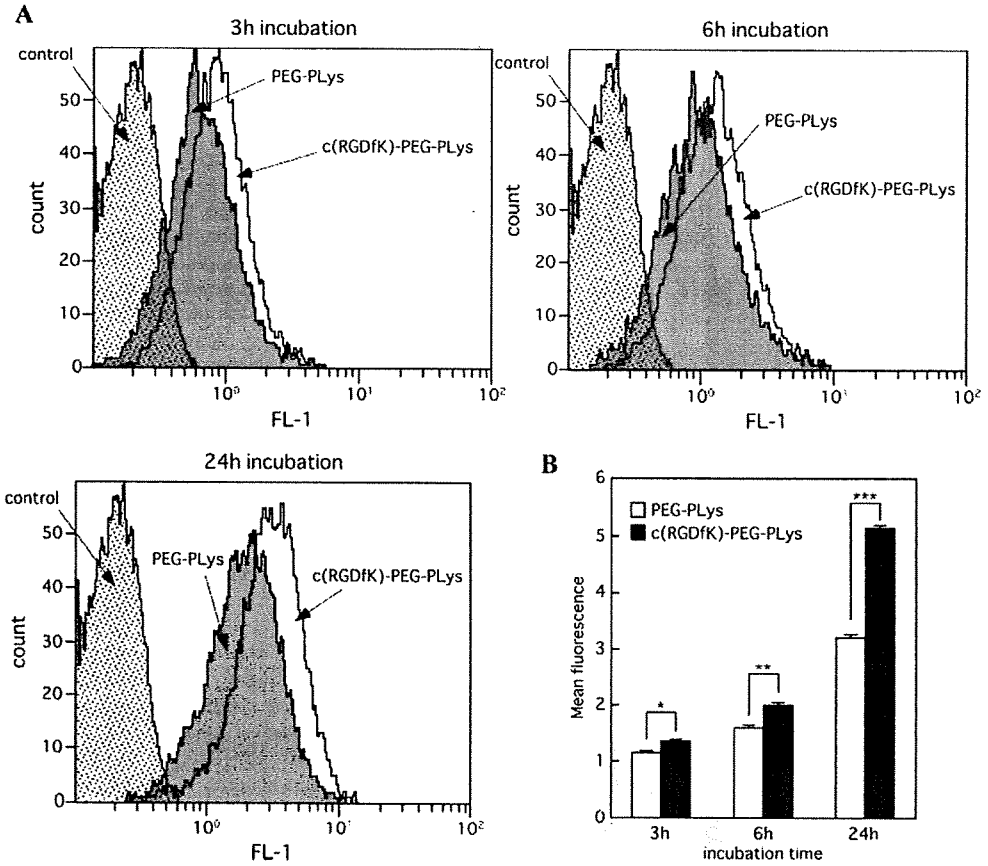

Figure 6. Cellular uptake of polyplex micelles. PEG−PLys and c(RGDfK)−PEG−PLys micelles loaded with fluorescein-labeled pDNA were applied to HeLa cells with varying incubation times. (A) Flow cytometric histogram profiles of time-dependent change in fluorescence intensity. (B) Mean fluorescence intensity at each incubation time. The data are the mean ± SEM, $n = 3$. $P^* < 0.05$, $P^{**} < 0.01$, and $P^{***} < 0.001$.

6) also suggests that the enhanced uptake of the c(RGDfK)−PEG−PLys/pDNA micelle might contribute to an increased TE against HeLa cells. Interestingly, the difference in the uptake ratio against the HeLa cells between the c(RGDfK) micelle and the ligand-free micelle became more significant with increased incubation time as seen in Figure 6. Integrin receptors are known to recycle to the plasma membrane through an endocytic cycle every 15−40 min (*27*). Consequently, this fast recycle of integrins might contribute to the facilitated uptake of the c(RGDfK) micelle into the HeLa cells in comparison with the ligand-free micelle. Nevertheless, as can be seen from Figures 5 and 6B, the uptake ratio is not simply correlated in a time-dependent manner with the TE. The ligand effect appeared to be more significant in the TE than in the uptake ratio, particularly after a prolonged time period such as 24 h. This result led us to assume that the c(RGDfK) ligand may also affect intracellular trafficking of the polyplex micelles. Indeed, a CLSM observation of HeLa cells challenged with polyplex micelles revealed a substantial difference in intracellular distribution between the PEG−PLys and c(RGDfK)−PEG−PLys micelles (Figure 7). In the cells challenged with the PEG−PLys polyplex micelle, a majority of pDNA was still distributed near the cell membrane, whereas in the same time frame of 3 h the cells with the c(RGDfK)−PEG−PLys polyplex micelle showed an appreciable accumulation of pDNA in the perinuclear region. It is noteworthy that a definite fraction of pDNA (colored red) in the perinuclear region did not co-localize with LysoTracker (colored green), suggesting that this fraction may be located in a compartment other than the acidic late endosome and lysosome. The $\alpha_v\beta_3$ integrin receptors have been reported to pass rapidly through the early endosomes, arriving at the perinuclear compartments approximately 30 min after internalization (*28*). Recent reports have shown an active transport pathway for a nonviral gene delivery system (*29*, *30*), in which microtubule-associated motor proteins have contributed to a rapid perinuclear accumulation of the polyplex within minutes after transfection. Also, recent studies have revealed that polyplexes in the perinuclear region but not in the acidic compartments significantly contribute to the effective transfection (*31*, *32*). These phenomena are consistent with our observation of a partial accumulation of the c(RGDfK)−PEG−PLys micelle in the perinuclear sites but outside of the acidic compartments, suggesting that the enhancement of the TE of the polyplex micelle by the introduction of cyclic RGD peptide ligands might be due not only to the enhanced uptake but also to the change in the intracellular trafficking route directed to the nucleus. It is likely that the micelle fraction distributed in nonacidic compartments near the nucleus may efficiently internalize into the nucleus when the cells are in the dividing phase, thus contributing to the increase in the transfection. Although the effective transport of the PLys-based polyplex micelles from the isolated compartment into the cytoplasm remains an issue because of inefficiency in the PLys function of facilitating the endosome-escaping step, the conjugation of c(RGDfK) ligands onto the polyplex micelle surface has great potential to improve the TE through modulated intracellular trafficking.

In conclusion, a successful synthetic route involving block copolymers conjugated with peptidyl ligands through thiazolidine ring formation was developed in this study. Cyclic RGD peptide-conjugated polyplex micelles showed an increased TE against HeLa cells possessing $\alpha_v\beta_3$ and $\alpha_v\beta_5$ integrins because

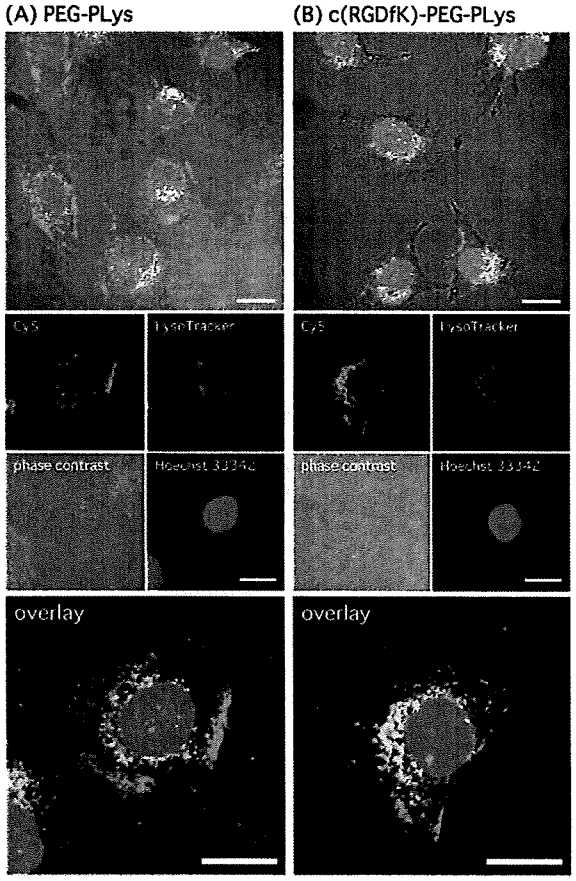

Figure 7. Intracellular distribution of pDNA challenged by the polyplex micelles. PEG−PLys and c(RGDfK)−PEG−PLys micelles loaded with Cy5-labeled pDNA (red) were incubated with HeLa cells for 3 h. The CLSM observation was performed using a 63× objective. The cell nuclei were stained with Hoechst 33342 (blue), and the acidic late endosome and lysosome were stained with LysoTracker Green (green). The scale bar represents 20 μm.

of enhanced uptake and a possible change in the route of intracellular trafficking. These results indicate that the introduction of various peptide ligands including c(RGDfK) peptide into the block copolymers is feasible and could eventually allow the construction of targetable polyplex micelles that are useful for site-specific gene therapy through a systemic route.

ACKNOWLEDGMENT

We thank Ms. K. Date (The University of Tokyo) and Ms. J. Kawakita (The University of Tokyo) for technical assistance. This work was financially supported in part by the Core Research Program for Evolutional Science and Technology (CREST) from Japan Science and Technology Corporation (JST) and the Project on the Materials Development for Innovative NanoDrug Delivery Systems from the Ministry of Education, Culture, Sports, Science and Technology (MEXT), Japan.

LITERATURE CITED

(1) Pedroso de Lima, M. C., Simoes, S., Pires, P., Faneca, H., and Düzgunes, N. (2001) Cationic lipid-DNA complexes in gene delivery: from biophysics to biological applications. *Adv. Drug Delivery Rev. 47*, 277−294.

(2) Merdan, T., Kopecek, J., and Kissel, T. (2002) Prospects for cationic polymers in gene and oligonucleotide therapy against cancer. *Adv. Drug Delivery Rev. 54*, 715−758.

(3) Kakizawa, Y., and Kataoka, K. (2002) Block copolymer micelles for delivery of gene and related compounds. *Adv. Drug Delivery Rev. 54*, 203−222.

(4) Itaka, K., Harada, A., Nakamura, K., Kawaguchi, H., and Kataoka, K. (2002) Evaluation by fluorescence resonance energy transfer of the stability of nonviral gene delivery vectors under physiological conditions. *Biomacromolecules 3*, 841−845.

(5) Harada-Shiba, M., Yamauchi, K., Harada, A., Takamisawa, I., Shimokado, K., and Kataoka, K. (2002) Polyion complex micelles as vectors in gene therapy-pharmacokinetics and in vivo gene transfer. *Gene Ther. 9*, 407−414.

(6) Wakebayashi, D., Nishiyama, N., Yamasaki, Y., Itaka, K., Kanayama, N., Harada, A., Nagasaki, Y., and Kataoka, K. (2004) Lactose-conjugated polyion complex micelles incorporating plasmid DNA as a targetable gene vector system: their preparation and gene transfecting efficiency against cultured HepG2 cells. *J. Controlled Release 95*, 653−664.

(7) Suh, W., Han, S.-O., Yu, L., and Kim, S. W. (2002) An angiogenic, endothelial-cell-targeted polymeric gene carrier. *Mol. Ther. 6*, 664−672.

(8) Ogris, M., Walker, G., Blessing, T., Kircheis, R., Wolschek, M., and Wagner, E. (2003) Tumor-targeted gene therapy: strategies for the preparation of ligand-polyethylene glycol-polyethylenimine/DNA complexes. *J. Controlled Release 91*, 173−181.

(9) Miyata, K., Kakizawa, Y., Nishiyama, N., Yamasaki, Y., Watanabe, T., Kohara, M., and Kataoka, K. (2005) Freeze-dried formulations for in vivo gene delivery of PEGylated polyplex micelles with disulfide crosslinked cores to the liver. *J. Controlled Release 109*, 15−23.

(10) Haubner, R., Gratias, R., Diefenbach, B., Goodman, S. L., Jonczyk, A., and Kessler, H. (1996) Structural and functional aspects of RGD-containing cyclic pentapeptides as highly potent and selective integrin $\alpha_v\beta_3$ antagonist. *J. Am. Chem. Soc. 118*, 7461−7472.

(11) Brooks, P. C., Clark, R. A. F., and Cheresh, D. A. (1994) Requirement of vascular integrin $\alpha_v\beta_3$ for angiogenesis. *Science 264*, 569−571.

(12) Akiyama, Y., Harada, A., Nagasaki, Y., and Kataoka, K. (2000) Synthesis of poly(ethylene glycol)-*block*-poly(ethylenimine) possessing an acetal group at the PEG end. *Macromolecules 33*, 5841−5845.

(13) Harada, A., and Kataoka, K. (1995) Formation of polyion complex micelles in an aqueous milieu from a pair of oppositely charged block copolymers with poly(ethylene glycol) segments. *Macromolecules 28*, 294−299.

(14) Nagasaki, Y., Kutsuna, T., Iijima, M., Kato, M., and Kataoka, K. (1995) Formyl-ended heterobifunctional poly(ethylene oxide): synthesis of poly(ethylene oxide) with a formyl group at one end and a hydroxyl group at the other end. *Bioconjugate Chem. 6*, 231−233.

(15) Poche, D. S., Moore, M. J., and Bowles, J. L. (1999) An unconventional method for purifying *N*-carboxyanhydride derivatives of γ-alkyl-L-glutamates. *Synth. Commun. 29*, 843−854.

(16) Zhang, L., Torgerson, T. R., Liu, X.-Y., Timmons, S., Colosia, A. D., Hawiger, J., and Tam, J. P. (1998) Preparation of functionally active cell-permeable peptides by single-step ligation of two peptide modules. *Proc. Natl. Acad. Sci. U.S.A. 95*, 9184−9189.

(17) LePecq, J.-B., and Paoletti, C. (1967) A fluorescent complex between ethidium bromide and nucleic acids. *J. Mol. Biol. 27*, 87−106.

(18) Itaka, K., Yamauchi, K., Harada, A., Nakamura, K., Kawaguchi, H., and Kataoka, K. (2003) Polyion complex micelles from plasmid DNA and poly(ethylene glycol)-poly(L-lysine) block copolymer as serum-tolerable polyplex system: physicochemical properties of micelles relevant to gene transfection efficiency. *Biomaterials 24*, 4495−4506.

(19) Wakebayashi, D., Nishiyama, N., Itaka, K., Miyata, K., Yamasaki, Y., Harada, A., Koyama, H., Nagasaki, Y., and Kataoka, K. (2004) Polyion complex micelles of pDNA with acetal-poly(ethylene glycol)-poly(2-(dimethylamino)ethyl methacrylate) block copolymer as the gene carrier system: physicochemical properties of micelles relevant to gene transfection efficiency. *Biomacromolecules 5*, 2128−2136.

(20) Pierschbacher, M. D., and Ruoslahti, E. (1984) Cell attachment activity of fibronectin can be duplicated by small synthetic fragments of the molecule. *Nature 309*, 30−33.

(21) Pierschbacher, M. D., and Ruoslahti, E. (1984) Variants of the cell recognition site of fibronectin that retain attachment-promoting activity. *Proc. Natl. Acad. Sci. U.S.A. 81*, 5985−5988.

(22) Dechantsreiter, M. A., Planker, E., Mathä, B., Lohof, E., Hölzemann, G., Jonczyk, A., Goodman, S. L., and Kessler, H. (1999) *N*-Methylated cyclic RGD peptides as highly active and selective $\alpha_v\beta_3$ integrin antagonists. *J. Med. Chem. 42*, 3033−3040.

(23) Allen, T. M. (2002) Ligand-targeted therapeutics in anticancer therapy. *Nat. Rev. 2*, 750−763.

(24) Kim, W. J., Yockman, J. W., Lee, M., Jeong, J. H., Kim, Y.-H., and Kim, S. W. (2005) Soluble *Flt-1* gene delivery using PEI-*g*-PEG-RGD conjugate for anti-angiogenesis. *J. Controlled Release 106*, 224−234.

(25) Kim, W. J., Yockman, J. W., Jeong, J. H., Christensen, L. V., Lee, M., Kim, Y.-H., and Kim, S. W. (2006) Anti-angiogenic inhibition of tumor growth by systemic delivery of PEI-*g*-PEG-RGD/pCMV-sFlt-1 complexes in tumor-bearing mice. *J. Controlled Release 114*, 381−388.

(26) Marinelli, L., Gottschalk, K.-E., Meyer, A., Novellino, E., and Kessler, H. (2004) Human integrin $\alpha_v\beta_5$: homology modeling and ligand binding. *J. Med. Chem. 47*, 4166−4177.

(27) Bretscher, M. S. (1996) Moving membrane up to the front of migrating cells. *Cell 85*, 465−467.

(28) Marnie, R., Simon, B., Alison, W., Peter, S., and Jim, N. (2001) PDGF-regulated rab4-dependent recycling of $\alpha_v\beta_3$ integrin from early endosomes is necessary for cell adhesion and spreading. *Curr. Biol. 11*, 1392−1402.

(29) Suh, J., Wirtz, D., and Hanes, J. (2003) Efficient active transport of gene nanocarriers to the cell nucleus. *Proc. Natl. Acad. Sci. U.S.A. 100*, 3878−3882.

(30) Kulkarni, R. P., Wu, D. D., Davis, M. E., and Fraser, S. E. (2005) Quantitating intracellular transport of polyplexes by spatio-temporal image correlation spectroscopy. *Proc. Natl. Acad. Sci. U.S.A. 102*, 7523−7528.

(31) Rejmna, J., Bragonzi, A., and Conese, M. (2005) Role of clathrin- and caveolae-mediated endocytosis in gene transfer mediated by lipo- and polyplexes. *Mol. Ther. 12*, 468−474.

(32) Gersdorff, K., Sanders, N. N., Vandenbroucke, R., Smedt, S. C., Wagner, E., and Ogris, M. (2006) The internalization route resulting in successful gene expression depends on both cell line and polyethylenimine polyplex type. *Mol. Ther. 14*, 745−753.

BC0700133

Available online at www.sciencedirect.com
ScienceDirect
Journal of Controlled Release 121 (2007) 38–48
journal of controlled release
www.elsevier.com/locate/jconrel

Transfection study using multicellular tumor spheroids for screening non-viral polymeric gene vectors with low cytotoxicity and high transfection efficiencies

Muri Han [a], Younsoo Bae [b,c], Nobuhiro Nishiyama [b,c,d], Kanjiro Miyata [c,e], Makoto Oba [f], Kazunori Kataoka [a,b,c,d,e,*]

[a] *Department of Materials Engineering, School of Engineering, The University of Tokyo, 7-3-1 Hongo, Bunkyo-ku, Tokyo 113-8656, Japan*
[b] *Center for Disease Biology and Integrative Medicine, School of Medicine, The University of Tokyo, 7-3-1 Hongo, Bunkyo-ku, Tokyo 113-0033, Japan*
[c] *Center for NanoBio Integration, The University of Tokyo, 7-3-1 Hongo, Bunkyo-ku, Tokyo 113-8656, Japan*
[d] *Core Research for Evolutional Science and Technology (CREST), Japan Science and Technology Agency (JST), Japan*
[e] *Department of Bioengineering, School of Engineering, The University of Tokyo, 7-3-1 Hongo, Bunkyo-ku, Tokyo 113-0033, Japan*
[f] *Department of Clinical Vascular Regeneration, School of Medicine, The University of Tokyo, 7-3-1 Hongo, Bunkyo-ku, Tokyo 113-8655, Japan*

Received 19 March 2007; accepted 8 May 2007
Available online 17 May 2007

Abstract

Polyplexes consisting of plasmid DNA and polycations have received much attention as promising vectors for gene transfer. For effective gene therapy, polycations with different polyamine structures in the side chain were developed to ensure their buffering capacity for endosomal escape, and their PEGylated block copolymers were developed to increase their stability and biocompatibility. The effects of the chemical structures of polycations and their PEGylation on transfection and cytotoxicity were elucidated by use of a three-dimensional multicellular tumor spheroid of human hepatoma HuH-7 cells. Various features of transfection with polyplex micelles, which have been hard to observe in conventional monolayer cultures, were revealed by the multicellular tumor spheroid (MCTS) model in terms of cytotoxicity and time-dependent behaviors of transfected gene expression under three-dimensional microenvironments. By using this system, the polyplex micelle from poly(ethylene glycol)-*b*-poly(*N*-substituted asparagine) copolymers having the *N*-(2-aminoethyl)-2-aminoethyl group in the side chain (PEG-*b*-P[Asp(DET)] polyplex micelle) was proved to achieve high transfection efficiencies as well as low cytotoxicity, both of which are critical properties for successful in vivo gene delivery.

Keywords: Non-viral gene vector; Block copolymer; Polyplex micelle; Spheroid

1. Introduction

A variety of non-viral polymeric gene vectors have received much attention in the past decade [1–3] for the delivery of genetic materials to the targeted cells in an effective and safe manner. Especially, the polyplexes formed by the electrostatic interaction between plasmid DNA (pDNA) and polycations have been designed to condense pDNA by shielding its negative charges, protect pDNA from rapid nucleolytic degradation, and facilitate its cellular uptake in order to achieve effective gene delivery [4–6]. It is well known that the chemical structures of polycations in polyplex systems play important roles in transfection efficiency. In this regard, polyethylenimine (PEI)-based polyplexes have been shown to be highly transfectable, presumably through the buffering of the endosomal cavity (i.e., so-called proton sponge effect) [2]. One of the advantages of polyplex systems is the possibility of various structural modifications to improve the stability and transfection efficiency of the polyplexes. Among such modifications, PEGylation [modification with poly(ethylene glycol)(PEG)] of polycations is a promising way to realize systemic gene delivery due to the improved stability of polyplexes in biological media [7–10].

* Corresponding author. Department of Materials Engineering, Graduate School of Engineering, The University of Tokyo, 7-3-1 Hongo, Bunkyo-ku, Tokyo 113-8656, Japan. Fax: +81 3 5841 7139.
E-mail address: kataoka@bmw.t.u-tokyo.ac.jp (K. Kataoka).

0168-3659/$ - see front matter © 2007 Elsevier B.V. All rights reserved.
doi:10.1016/j.jconrel.2007.05.012

A typical PEGylated polyplex is a core-shell type polyplex (polyplex micelle) formed through the electrostatic interaction between pDNA and PEG-*block*-polycation copolymers. Polyplex micelles have been demonstrated to show high colloidal stability under biological media and substantial transfection activity against various cells even after preincubation with serum proteins [11,12]. Moreover, polyplex micelles showed prolonged blood circulation and in vivo gene transfer to liver [5,13]. The chemical structures of polycations in block copolymers substantially affect the capability of polyplexes as efficient gene vectors. In this regard, we recently reported the development of highly transfectable but remarkably low cytotoxic PEG-*block*-polycation copolymers: PEG-*b*-poly(*N*-substituted asparagine) copolymers having the *N*-(2-aminoethyl)-2-aminoethyl group in the side chain (PEG-*b*-P[Asp(DET)]) [14]. Polyplex micelles from PEG-*b*-P[Asp(DET)] showed efficient and non-toxic transfection to several primary cells including endothelial and smooth muscle cells, which are sensitive to the polyplex-induced cytotoxicity, and successful gene transfection in vivo to vascular lesions [15]. Thus, the PEG-*b*-P[Asp(DET)] polyplex micelle is expected to be a potent non-viral vector for in vivo gene delivery.

The unique feature of the PEG-*b*-P[Asp(DET)] polyplex micelle to achieve appreciably high transfection efficacy with substantially lowered toxicity motivated us to further clarify the effects of PEGylation and the chemical structures of polyasparagine-based polyplexes on their transfection and cytotoxic behaviors. For this purpose, we have compared here two types of polyasparagine-based polycations having a subtle difference in the number of methylene units in the side chain: *N*-(2-aminoethyl)-2-aminoethyl group (P[Asp(DET)]) and *N*-(3-aminopropyl)-3-aminopropyl group (P[Asp(DPT)]). Furthermore, to explore the effect of PEGylation on polyplex behavior, two types of PEG-*b*-cationic polyasparagines, PEG-*b*-P[Asp(DET)] and PEG-*b*-P[Asp(DPT)], were prepared for the construction of polyplex micelles (Scheme 1). The transfection activity and cytotoxicity of polyplexes and polyplex micelles were evaluated with multicellular tumor spheroids (MCTS) as well as conventional monolayer culture cells. We focus on MCTS here because they are known to be very useful three-dimensional in vitro tumor models, representing morphological and functional features of in vivo avascular solid tumors, and because they are characterized by prolonged viable spans with actively proliferating outer cell layers [16]. Recently, Mellor et al. applied the transfection of polyethylenimine-based polyplexes to the MCTS with the relatively large size (~474 μm) to assess the penetration of the polyplexes inside the spheroids, approaching the issue of polyplex percolation in actual in vivo tissues [17]. In the present study, we focused on the MCTS with the relatively small size due to our finding that the size of MCTS is highly sensitive to polyplex-induced cytotoxicity; MCTS of approximately 100 μm showed even higher sensitivity than monolayered culture cells, probably due to their immature development of cell–cell and cell–extracellular matrix (ECM) interactions. Worth noting is that the prolonged viable span of MCTS allowed long-term evaluation of more than 10 days of the expression of transfected genes. These properties of MCTS models enabled us to evaluate polyplex systems under conditions close to those of in vivo solid tumors, revealing the excellent biocompatibility and durable gene expression behaviors of PEG-*b*-P[Asp(DET)] polyplex micelles.

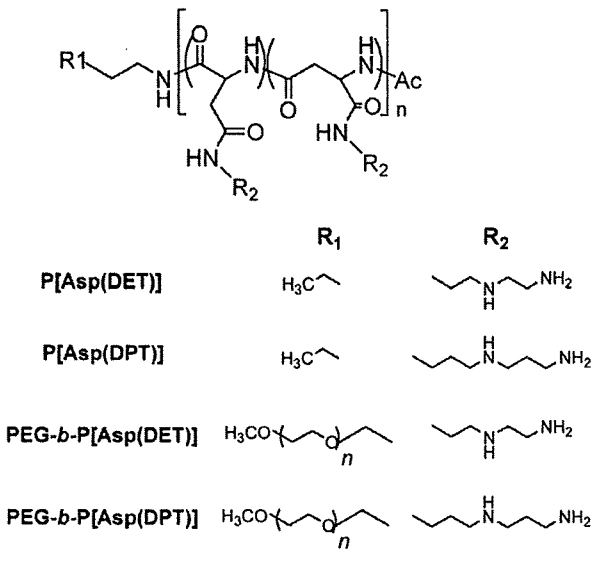

Scheme 1. Chemical structures of polycations.

2. Experimental

2.1. Materials

β-Benzyl-L-aspartate *N*-carboxyanhidride (BLA-NCA) and α-methoxy-ω-amino poly(ethylene glycol) (MeO-PEG-NH_2) (M_r=12,000) were obtained from Nippon Oil and Fats Co., Ltd. (Japan). Diethylenetriaimine (DET) and dipropylenetriamine (DPT) were purchased from Tokyo Kasei Kogyo Co., Ltd. (Japan) and distilled over CaH_2 under reduced pressure. *N,N*-Dimethylformamide (DMF), dichloromethane, and acetic anhydride were purchased from Wako Pure Chemical Industries, Ltd. (Japan) and purified by general methods before use. Linear polyethylenimine (ExGen 500 in vitro transfection reagent, 22 KDa) and branched polyethylenimine (25 KDa) were purchased from Fermentas (Canada) and Aldrich (USA), respectively.

2.2. Synthesis of poly(N-substituted asparagines) and their block copolymers with poly(ethylene glycol) (PEG)

The PEG-*block*-poly(β-benzyl L-aspartate) (PEG-*b*-PBLA) was prepared as previously reported [14]. Briefly, BLA-NCA was polymerized in DMF at 40 °C from the terminal primary amino group of MeO-PEG-NH_2, followed by the acetylation of the *N*-terminus of PBLA by acetic anhydride to obtain PEG-*b*-PBLA-Ac. PEG-*b*-PBLA-Ac was confirmed to have a unimodal molecular weight distribution (M_w/M_n: 1.17) by gel-permeation chromatography (GPC) measurement [columns: TSK-gel G4000HHR+G3000HHR, eluent: DMF+10 mM LiCl, T=40 °C, detector: Refractive Index (RI)] (data not shown).

The degree of polymerization (DP) of PBLA was calculated to be 101 based on ^{1}H NMR spectroscopy (data not shown).

Lyophilized PEG-*b*-PBLA (300 mg, 11.6 μmol) was dissolved in DMF (10 mL), followed by the reaction with DET (50 equiv to benzyl group of PBLA segment, 4.0 g, 39.4 mmol) under mild anhydrous conditions to obtain PEG-*b*-P[Asp(DET)]. After 24 h, the reaction mixture was slowly added dropwise into a solution of acetic acid (10% *v/v*, 40 mL) and dialyzed against a solution of 0.01 N HCl and then distilled water (M_r cutoff: 3500 Da). The final solution was lyophilized to obtain the polymer as the chloride salt form, and the yield was approximately 90%. Similarly, PEG-*b*-P[Asp(DPT)] was synthesized by the aminolysis reaction of PEG-*b*-PBLA-Ac with DPT. The structures of these block catiomers were confirmed by ^{1}H and ^{13}C NMR measurements.

Cationic homopolymers, P[Asp(DET)] and P[Asp(DPT)], were synthesized by the aminolysis reaction of PBLA homopolymer [degree of polymerization (DP): 98], which was obtained by the polymerization of BLA-NCA initiated by *n*-butylamine. The unimodal distribution and the almost 100% conversion of the BLA side chains of these homopolymers into the desired amino groups were confirmed by GPC and ^{1}H NMR measurements, respectively.

2.3. Titration of polymers

Each homopolymer (68 mg of P[Asp(DET)] and 75 mg of P[Asp(DPT)]) or block copolymer (98 mg of PEG-*b*-P[Asp(DET)] and 104 mg of PEG-*b*-P[Asp(DPT)]) was dissolved in 40 mL of 0.005 N HCl with 150 mM NaCl, and titrated with 0.05 N NaOH with 150 mM NaCl at 37 °C. An automatic titrator (TITSTATION TS-2000, Hiranuma Co., Ltd., Kyoto, Japan) was used for the titration. In this experiment, the titrant was added in 0.0315 mL quantities after the confirmation that the pH values became stable (minimal interval: 30 s). The pH-α curves were determined from the obtained titration curve. For the estimation of the charge in the protonation affinity with α apparent $pK(=pH+\log[\alpha/(1-\alpha)])$ was plotted against $1-\alpha$, where K is the effective dissociation constant.

2.4. Plasmid DNA

The plasmid, pCAcc vector having CAG promoter [18], was provided by RIKEN Bioresource Center (Japan). Also, a fragment cDNA of SEYFP-F46L (*Venus*), which is a variant of yellow fluorescent protein with the mutation F46L [19], was provided by Dr. A. Miyawaki at the Brain Science Institute, RIKEN (Japan) and inserted into the pCAcc vector (pCAcc+*Venus*). Each plasmid DNA (pDNA) was amplified in competent DH5α *Escherichia coli* and purified using HiSpeed Plasmid MaxiKit (QIAGEN Sciences Co., Inc., Germany). The pDNA concentration was determined by the absorption at 260 nm.

2.5. Preparation of the polyplexes

Poly(ethylene glycol)-*block*-polycation copolymer and pDNA were first separately dissolved in 10 mM Tris–HCl buffer (pH 7.4). Then, both solutions were mixed at various ratios of the number of amino group (primary and secondary amino groups) units per nucleotide (*N/P* ratios). The final pDNA concentration of the mixture was adjusted to 100 μg/mL. Polyplex micelle was applied to each well for transfection after overnight incubation at ambient temperature. Polyplex was prepared similarly by mixing cationic homopolymer and pDNA solution. Polyplex was applied to each well for transfection after 30 min of incubation at ambient temperature.

2.6. In vitro transfection to HuH-7 cells

For the monolayer culture study, human hepatoma HuH-7 cells were seeded on 24-well culture plates and incubated overnight in 400 μL of Dulbecco's modified eagle's medium (DMEM) containing 10% fetal bovine serum (FBS) before transfection. Then, 10 μL of each polyplex solution was applied to each well for the transfection. The amount of pDNA was adjusted to 1 μg per well. After 24 h of incubation, the medium was replaced with 400 μL of the medium containing 10% serum, followed by an additional 24 h of incubation. The luciferase gene expression was then evaluated using the Luciferase Assay System (Promega, USA) and a Lumat LB9507 luminometer (Berthold Technologies, Germany). The amount of protein in each well was concomitantly determined using a Micro BCA Protein Assay Reagent Kit. To prepare MCTS, 200 μL of cell suspension (2×10^2 cell/ml) was seeded into a 96-well culture plate designed for spheroid formation (SUMILONCELLTIGHT, Sumitomo Bakelite Co., Ltd., Japan). After 48 h of incubation, a multicellular spheroid with diameter of ca 100 μm was spontaneously formed in each well. Then, 10 μL of each polyplex solution was applied to each well for the transfection. The amount of pDNA was adjusted to 1 μg per well. After 24 h of incubation, the medium was replaced with 200 μL of the medium containing 10% serum, followed by an additional 24 h of incubation. During the incubation period, the medium was replaced by fresh medium containing 10% serum every 3 days. The *Venus* gene expression was then evaluated using an LSM 510 confocal microscope (Carl Zeiss, Germany; excitation wavelength: 488 nm).

2.7. Live/dead assay

Live and Dead assay was accomplished with the Live/Dead kit protocol (Molecular Probes, USA) against cultured spheroids. Spheroids were rinsed with PBS (−) and then incubated with a solution containing 0.8 μM calcein AM (excitation 495 nm, emission 515 nm) and 4 μM EthD-1 (excitation 495 nm, emission 635 nm) in PBS (−) for 3 h at 37 °C, followed by observation through a Carl Zeiss LSM 510 confocal laser scanning microscope. The concentration and incubation time were optimized to allow the selective labeling of HuH-7 spheroids between live and dead cells.

2.8. Fluorescence measurements

For observation of the gene expression of the fluorescent protein *Venus*, MCTS samples were rinsed and mounted in PBS (−), and then observed by confocal microscope. The LSM 510

laser scanning microscope was used for the optical sectioning of the spheroids. An argon gas laser with an excitation wavelength of 488 nm was used to emit the fluorescence of the YFP.

2.9. Cell viability assay

Cell viability assay was accomplished with a protocol (CellTiter-Glo®Luminescent Cell Viability Assay, Promega, USA) against cultured cells. After 24 h incubation of HuH-7 cells in opaque 24-well plates, the polyplex to be tested was added. The cells were rinsed with PBS (−) after 24 h of incubation, then 200 μL of reagent to an equal volume of cell culture medium was added to each well. After mixing for 2 min, the plate was incubated at room temperature for 10 min. The luminescence was evaluated using a Lumat LB9507 luminometer (Berthold Technologies, Germany).

2.10. Quantification of gene expression in MCTS

The total intensity was calculated from the piled up fluorescence images of fluorescence of *Venus* from each optical slice (at a depth of 1 μm) by Imaris® software in combination with Imaris MeasurementPro (Carl Zeiss, Germany), which enables the measurement of the intensity value for groups of selected voxels. The relative intensity was determined from the total intensity of one spheroid divided by a volume of spheroid.

2.11. Dissociation of P[Asp(DET)] polyplex and PEG-b-P[Asp(DET)] micelle

The release of pDNA from the complexes was evaluated through the exchange reaction with an anionic lipid, 1,2-dioleoyl-*sn*-glycero-3-phospho-L-serine sodium salt (DOPS, Sigma). Two mg/mL of DOPS solution was added to the P[Asp(DET)] polyplex and to the PEG-*b*-P[Asp(DET)] polyplex micelle solutions prepared at the *N/P* ratio of 20 to obtain mixed solutions with varying unit molar ratios ([carboxyl groups in DOPS]/[phosphate groups in pDNA]). The final pDNA concentration was adjusted to 16.7 μg/mL. After overnight incubation at 25 °C, the mixed solutions were electrophoresed with 0.9 wt.% agarose gel in the buffer (3.3 mM Tris–acetic acid (pH 7.4)+1.7 mM sodium acetate+1 mM EDTA2Na). pDNAs in the gel were visualized by soaking the gel in an ethidium bromide solution (0.5 mg/L) and analyzed using a Luminous Imager V5 (AISIN SEIKI Co., Ltd., Japan).

3. Results

3.1. Protonation behaviors of polycations and their block copolymers with PEG

In this study, sets of cationic poly(*N*-substituted asparagine) homopolymers and PEG-*b*-poly(*N*-substituted asparagine) copolymers having the *N*-(2-aminoethyl)-2-aminoethyl group (P[Asp(DET)]) or the *N*-(3-aminopropyl)-3-aminopropyl group (P[Asp(DPT)]) in the side chain (Scheme 1) were prepared to study the effects of the chemical structures of polycations as well as the PEGylation of polycations on the properties of polyplex components. This synthetic method is based on our finding that the flanking benzyl ester groups of PBLA undergo a quantitative aminolysis reaction with various polyamine compounds under careful anhydrous conditions, so that a series of polymers has the same polymerization degree and distribution [14], allowing a direct comparison of subtle changes in their chemical structures.

The pH-dependent protonation behaviors of the obtained homopolymers, P[Asp(DET)] and P[Asp(DPT)], in 150 mM NaCl-containing media at 37°C seemed to be clearly distinct as shown in Fig. 1A. Indeed, P[Asp(DET)] displayed two-step protonation behavior and the protonation degree (α) of 0.53 at pH 7.4, whereas the protonation of P[Asp(DPT)] did not show clear two-step protonation and showed a higher protonation degree (α=0.88) at pH 7.4. From the p*K*–α curve (data not shown), the pK_1 (p*K* at α=0.25) and pK_2 (p*K* at α=0.75) of P[Asp(DET)] were calculated as 9.1 and 6.3, respectively, and the pK_1 and pK_2 of P[Asp(DPT)] were also calculated as 9.7 and 8.6, respectively. The two distinct p*K* values (pK_1 and pK_2) correspond to the first and

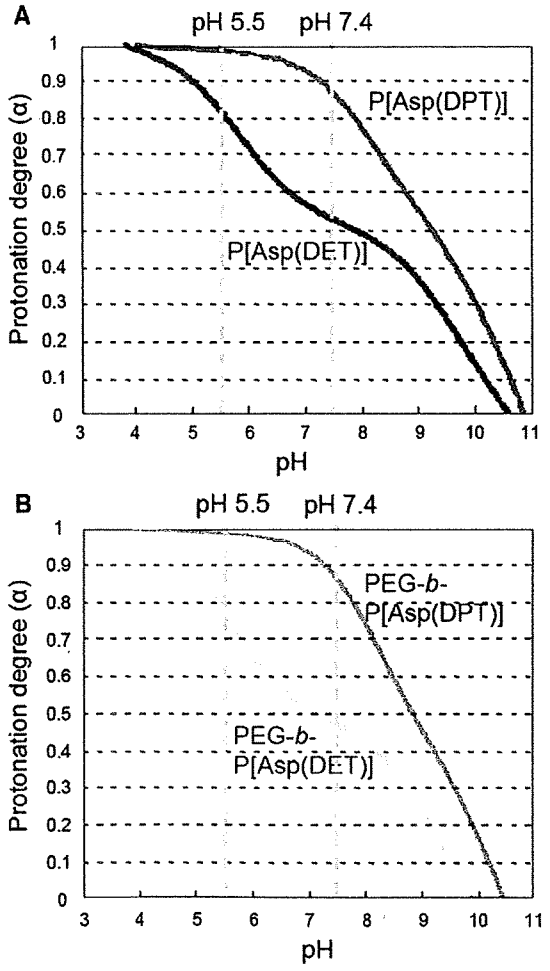

Fig. 1. pH–α (protonation degree) curves of P[Asp(DET)] and P[Asp(DPT)] (A) and PEG-*b*-P[Asp(DET)] and PEG-*b*-P[Asp(DPT)] (B) (37 °C, 150 mM NaCl, 0.05 M NaOH as titrant, 0.5 mmol amine concentration).

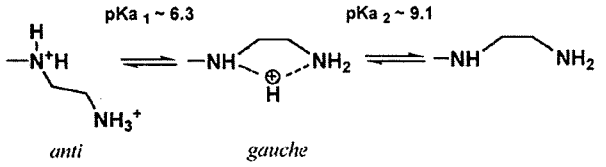

Scheme 2. Two-step protonation of ethylenediamine side chain of P[Asp(DET)].

second protonation steps of diamine units, respectively, in the side chain. Consequently, P[Asp(DET)] might exert a substantial buffering capacity in the pH range from 7.4 to 5.0, leading presumably to potent transfection activity based on the proton sponge effect. It is noteworthy that P[Asp(DET)] has a two orders of magnitude higher proton dissociation constant (or lower protonation constant) for the second protonation than P[Asp(DPT)], indicating that the former is less favorable than the latter to the double-protonated state. This may be due to the strong electrostatic repulsion between two protonated amines in ethylenediamine units of P[Asp(DET)] to take only the *anti*-conformation (Scheme 2). As seen in the case of P[Asp(DPT)], an increase in one more unit of the methylene group between two amino groups in the side chain effectively reduces the electrostatic repulsion to facilitate the protonation.

pH-α curves of PEG-*b*-poly(*N*-substituted asparagine) (PEG-*b*-P[Asp(DET)] and PEG-*b*-P[Asp(DPT)]) were also shown in Fig. 1B, showing a tendency similar to those of the homopolymers in Fig. 1A. From these results, the pK_1 and pK_2 of PEG-*b*-P[Asp(DET)] were calculated as 8.5 and 6.2, whereas the pK_1 and pK_2 of PEG-*b*-P[Asp(DPT)] were calculated as 9.3 and 8.5, respectively. It is noted that PEGylation of the polycations decreased the p*K* values, suggesting that PEGylation might prevent the protonation of polycations. Presumably, this might be explained by the decrease in the local permittivity of polycations caused by surrounding PEG chains.

3.2. Transfection efficiencies and cytotoxicity of polyplexes against monolayer cultured cells

The transfection efficiencies of cationic homopolymers/pDNA polyplexes against monolayer cultured HuH-7 cells were evaluated. The results of transfection after 48 h incubation (24 h incubation with the polyplexes followed by 24 h post-incubation after medium replacement) are shown in Fig. 2A. P[Asp(DET)] polyplexes showed high transfection efficiencies over the range of *N/P* ratios tested in this study. Especially, they displayed comparable or even higher transfection efficiencies at *N/P*=20 and 40 compared with LPEI and BPEI polyplexes [*N/P*=6 for LPEI according to the manufacturer's recommendation and *N/P*=10 for BPEI by optimization], which have been widely used in experimental transfection. P[Asp(DPT)] polyplexes showed appreciable transfection efficiency at *N/P*=10; however, the efficiency decreased at *N/P*=20 and 40, probably due to the emergence of significant cytotoxicity (Fig. 3).

Regarding the cytotoxicity of the polyplexes from cationic homopolymers (Fig. 3), both LPEI and BPEI polyplexes induced significant decreases in cell viability even at the *N/P* ratio appropriate for transfection. Polyplexes from P[Asp(DET)] were significantly less cytotoxic than the other polyplexes, whereas P[Asp(DPT)] polyplexes turned out to be highly cytotoxic. Thus, a subtle change in the chemical structure of the side chain of poly(*N*-substituted asparagine) unprecedentedly affected the cytotoxicity of the polyplexes.

In the cases of polyplex micelles from the block catiomers, PEG-*b*-P[Asp(DET)] polyplex micelles showed much better transfection efficiencies than PEG-*b*-P[Asp(DPT)] polyplex micelles (Fig. 2B), as was the case with the polyplexes from the corresponding homopolymers. With an increase in *N/P* ratio, each polyplex micelle showed an increase in transfection activity. Regarding cytotoxicity (Fig. 3), the PEG-*b*-P[Asp(DET)] polyplex micelles always displayed lower cytotoxicity than the

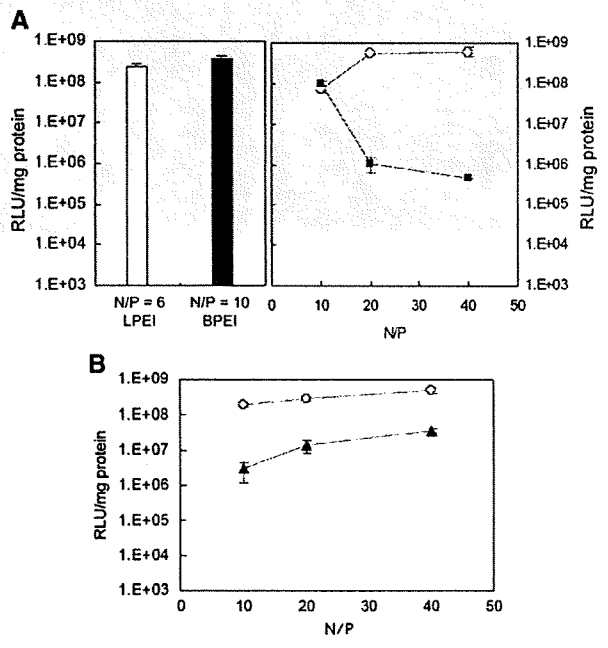

Fig. 2. The transfection of luciferase reporter gene against monolayer cultures of HuH-7. A) Transfection results with L/BPEI polyplexes (*N/P*=6 for LPEI according to the manufacturer's recommendation and *N/P*=10 for BPEI by optimization), P[Asp(DET)] polyplexes (○) and P[Asp(DPT)] polyplexes (■). B) Transfection results with PEG-*b*-P[Asp(DET)] polyplex micelles (○) and PEG-*b*-P[Asp(DPT)] polyplex micelles (▲).

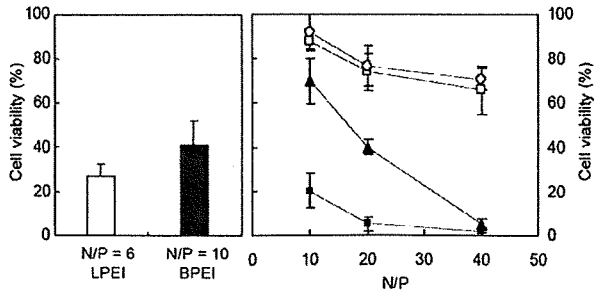

Fig. 3. Cytotoxicity of L/BPEI polyplexes (*N/P*=6 for LPEI according to the manufacturer's recommendation and *N/P*=10 for BPEI by optimization), P[Asp(DET)] polyplexes (□), P[Asp(DPT)] polyplexes (■), PEG-*b*-P[Asp(DET)] polyplex micelles (○), and PEG-*b*-P[Asp(DPT)] polyplex micelles (▲) toward HuH-7 cells after 48 h incubation.

PEG-*b*-P[Asp(DPT)] polyplex micelles at the same *N/P* ratios, and the difference in their cytotoxicity between these polyplex micelles became progressively more significant with increases in the *N/P* ratios. The cell viability remained high, and at levels similar between P[Asp(DET)] polyplexes and PEG-*b*-P[Asp (DET)] polyplex micelles, even with increased *N/P* ratios. This result suggests that the P[Asp(DET)] structure may have an inherently low cytotoxicity, which was further confirmed by the cytotoxicity assay of free polymers (Supporting Information 1). Notably, PEGylation significantly decreased the cytotoxicity of P[Asp(DPT)], resulting in improved transfection efficacy particularly at higher *N/P* ratios. This result clearly indicates that PEGylation is an efficient way to improve the compliance of a polyplex system involving cytotoxic polycations as a component [20]. Nevertheless, the PEGlyation of P[Asp(DET)] did not show any significant effect on cytotoxicity, apparently due to the minimally cytotoxic nature of the P[Asp(DET)] structure.

3.3. Evaluation of characteristic properties of MCTS

Fig. 4 shows the growth of HuH-7 MCTS from the initial diameter of 100 μm. By using Live/Dead assay (live cells: green fluorescence; dead cells: red fluorescence), necrosis of the inner cells of MCTS was observed by a confocal laser scanning microscope (CLSM) when the diameter reached around 400–500 μm (6–8 days after incubation). The necrotic region expanded along with the growth of MCTS. Thus, HuH-7 MCTS clearly took a heterogeneous structure according to the distance from the outer cell layers after they grew beyond the diffusion limit of oxygen and nutrition. Such a growth property represents a good in vitro model for the heterogeneity of solid tumors as a result of the inefficient vascular function [21,22].

3.4. Transfection efficiencies and cytotoxicity of polyplexes and polyplex micelles against MCTS

The gene expression of fluorescent protein *Venus* at defined time periods after transfection with the polyplexes or polyplex micelles was observed by CLSM as shown in Fig. 5. The spheroid diameter at the time of transfection was adjusted to 100 μm to ensure the long-term observation of the transfected gene expression within the optically observable depth range by CLSM. Under this condition, gene expression continued for over 10 days after the transfection and in some cases continued for over 1 month (data not shown). Images of the localization of transfected protein *Venus* in MCTS were taken from the upper surface going towards the center of the MCTS by the z-axis at 1–2 μm intervals of optical slices. Fig. 5A shows typical images of transfected *Venus* in MCTS at different *z*-axes (different distances from the spheroid surface) at 8 days after transfection with PEG-*b*-P[Asp(DET)] polyplex micelles (*N/P*=40). The images clearly showed that *Venus* was expressed even at the inner region of MCTS where necrosis was considered to be developed at the corresponding size (Fig. 4).

All the MCTS structures were destroyed after transfection with LPEI or BPEI polyplexes due to their toxicity even at low

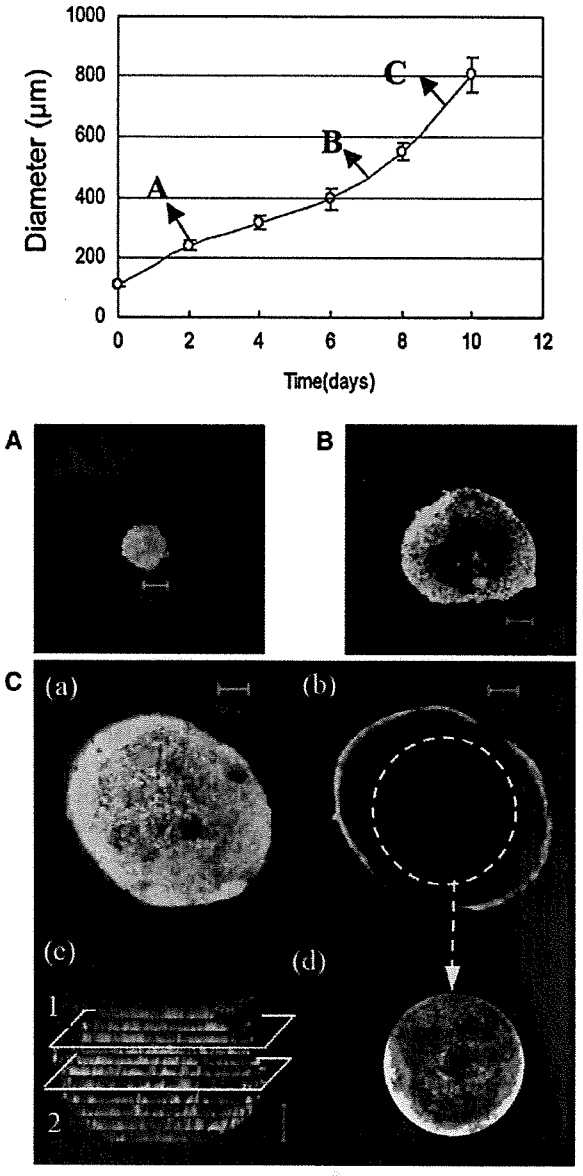

Fig. 4. Growth curve of HuH-7 spheroids and Live/Dead assay of spheroid at each time point of incubation (initial diameter is ca 100 μm. Optical slice at the middle of spheroid. Bar=100 μm. Green and red fluorescence from live and dead cells, respectively). A) 2 days after the formation of MCTS. B) 7 days after the formation of MCTS. C) 9 days after the formation of MCTS. In C, (a) optical slice of spheroid at position 1 of (c); (b) optical slice of spheroid at position 2 of (c); (c) side view of spheroid*; (d) retaken image of region of interest (ROI)**. (*This image was constructed by piling up side views. **This image was taken by stimulating the radiation of ROI by the amplification of laser.)

N/P ratios, and thus no systematic data on the spheroid transfection were obtained. P[Asp(DPT)] polyplexes also induced the destruction of MCTS in the whole range of *N/P* ratios tested in this study (*N/P*= 10, 20, and 40). By contrast, P [Asp(DET)] polyplexes showed successful transfection without destruction of the MCTS structure at *N/P* ratios of 10 and 20, as seen in Fig. 5B, highlighting the lower cytotoxicity of P[Asp (DET)] compared with P[Asp(DPT)], LPEI, and BPEI. Here,

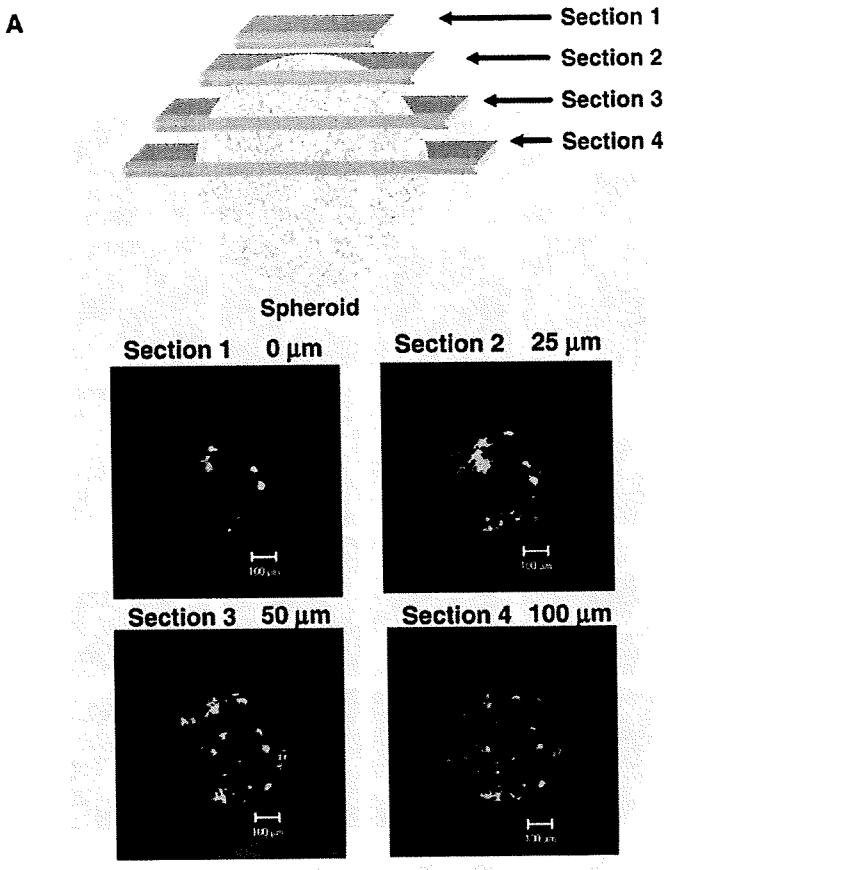
A
Section 1
Section 2
Section 3
Section 4
Spheroid
Section 1 0 μm
Section 2 25 μm
Section 3 50 μm
Section 4 100 μm

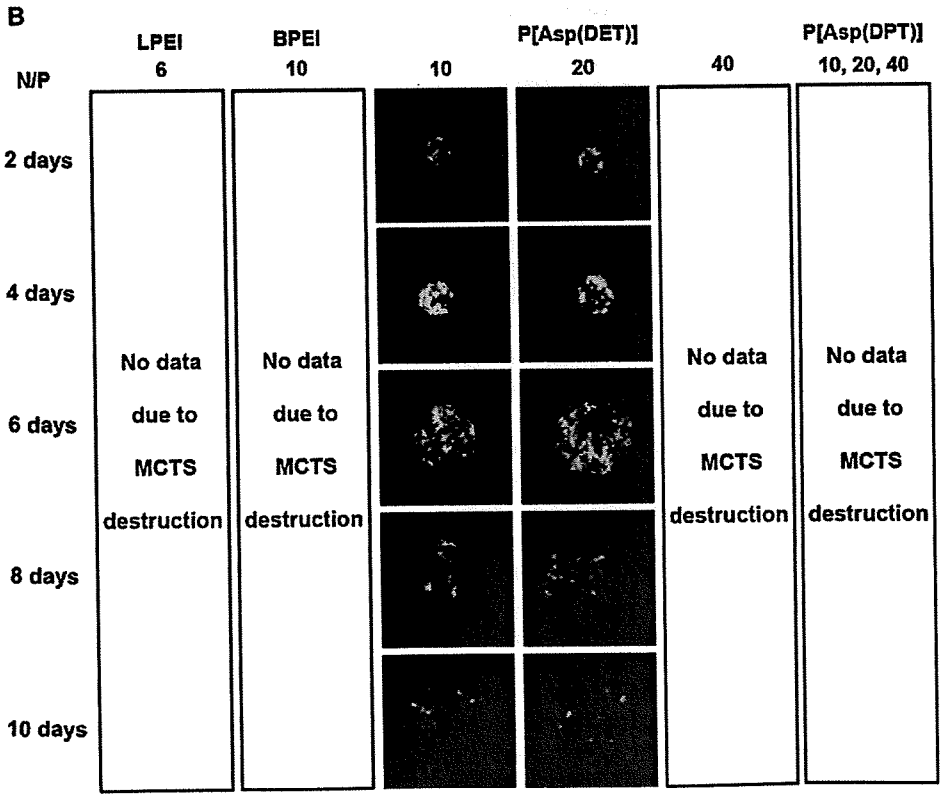
B
LPEI
BPEI
P[Asp(DET)]
P[Asp(DPT)]
N/P
6
10
10
20
40
10, 20, 40
2 days
4 days
6 days
8 days
10 days
No data due to MCTS destruction
No data due to MCTS destruction
No data due to MCTS destruction
No data due to MCTS destruction

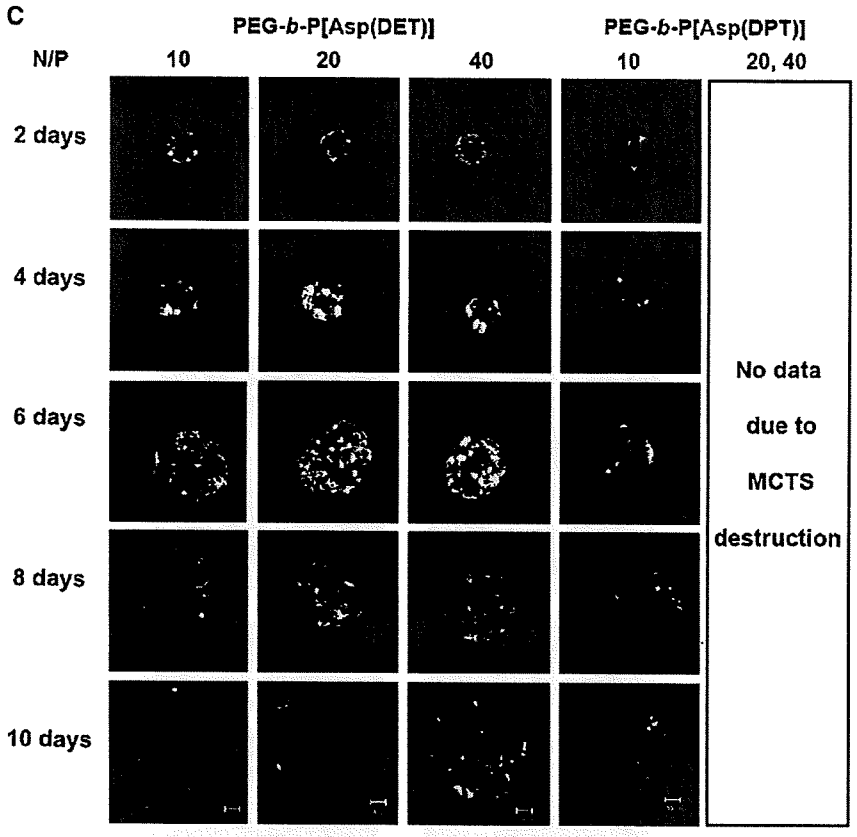

Fig. 5. Expression of marker protein *Venus* in HuH-7 spheroids (initial diameter is ca 100 μm. Bar=100 μm). A) Localization of transfected *Venus* by PEG-*b*-P[Asp(DET)] polyplex micelles according to the distance from the surface of the spheroid. (The images were the optical slices taken from the upper surface toward the center of the MCTS by the *z*-axis at 0, 25, 50, and 100 μm). B) Optical slices at the middle of spheroids with transfected protein *Venus* by P[Asp(DET)] and P[Asp(DPT)] polyplexes. (Results were not obtained due to the destruction of spheroids after transfection in the cases of *N/P*=4, 6, 8, 10 for LPEI, *N/P*=10, 20, 40 for BPEI, *N/P*=40 for P[Asp(DET)], *N/P*=10, 20, 40 for P[Asp(DPT)]). C) Optical slices at the middle of spheroids with transfected protein *Venus* by PEG-*b*-P[Asp(DET)] and PEG-*b*-P[Asp(DPT)] polyplex micelles. (Results were not obtained due to the destruction of spheroids after transfection in the cases of *N/P*=20, 40 for PEG-*b*-P[Asp(DPT)].)

the MCTS images at the middle section by the *z*-axis are shown for each day period. However, even P[Asp(DET)] polyplexes showed the destruction of spheroid structures by increasing the *N/P* ratio to 40.

Overall, PEG-*b*-P[Asp(DET) polyplex micelles showed better transfection activity than PEG-*b*-P[Asp(DPT)] polyplex micelles in MCTS, in agreement with the results of monolayer culture (Fig. 2B). PEG-*b*-P[Asp(DET)] polyplex micelles showed successful activity of the transfection without destruction of MCTS across the range of *N/P* ratios tested in this study (*N/P*=10, 20, and 40) (Fig. 5C). Worth mentioning is that PEG-*b*-P[Asp(DET)] polyplex micelles did not induce the destruction of spheroids even at *N/P*=40, where the MCTS structures were destroyed by the transfection with P[Asp(DET)] polyplexes (Fig. 5B) at that *N/P* ratio. Such reduction of cytotoxicity by PEGylation of polycations were not detected by the conventional monolayer culture study (Fig. 3, Supporting Information 1), highlighting high sensitivity of MCTS against polyplex-induced cytotoxicity. While the transfection efficiency of P[Asp(DPT)] was not obtained due to the destruction of MCTS after the transfection, the effect of PEGylation on reducing toxicity was remarkable in this case. Eventually, PEG-*b*-P[Asp(DPT)] polyplex micelles showed appreciable transfection efficiency at the *N/P* ratio of 10.

3.5. Time-dependent gene expression in MCTS

The total fluorescence intensity by *Venus* expression in MCTS was calculated by integrating the intensity image of each optical slice taken from the upper surface going towards the center of the MCTS by the *z*-axis at 1–2 μm intervals (Fig. 5A) using Imaris® software (Fig. 6A). The gene expression by the P[Asp(DET)] polyplexes (*N/P*=10 and 20) and PEG-*b*-P[Asp(DET)] polyplex micelles (*N/P*=10, 20, and 40), which showed successful transfection to MCTS, was quantified in this manner at each day period, and the results are shown in Fig. 6B. For both the polyplexes and polyplex micelles, increased the *N/P* ratios led to increased total intensities. Moreover P[Asp(DET)] polyplexes apparently had higher total intensities than PEG-*b*-P[Asp(DET)] polyplex micelles. The total intensity peaked at 6 days after transfection for all the polyplexes and polyplex micelles. It should be noted that such prolonged gene

expression is difficult to detect by the conventional monolayer culture study, because the monolayer cultured cells become confluent until 4 days, beyond which cell viability decreases remarkably. We also evaluated the relative intensity (=total intensity/volume of spheroid) of the expressed *Venus* in the spheroids transfected with the polyplexes or polyplex micelles (Fig. 6C) to normalize the differences in the growth rate and eventually the volume of each spheroid. Although the relative intensity of P[Asp(DET)] polyplexes decreased continuously with time, PEG-*b*-P[Asp(DET)] polyplex micelles with *N/P* ratios of 20 and 40 showed increased relative intensities until 4 days after transfection.

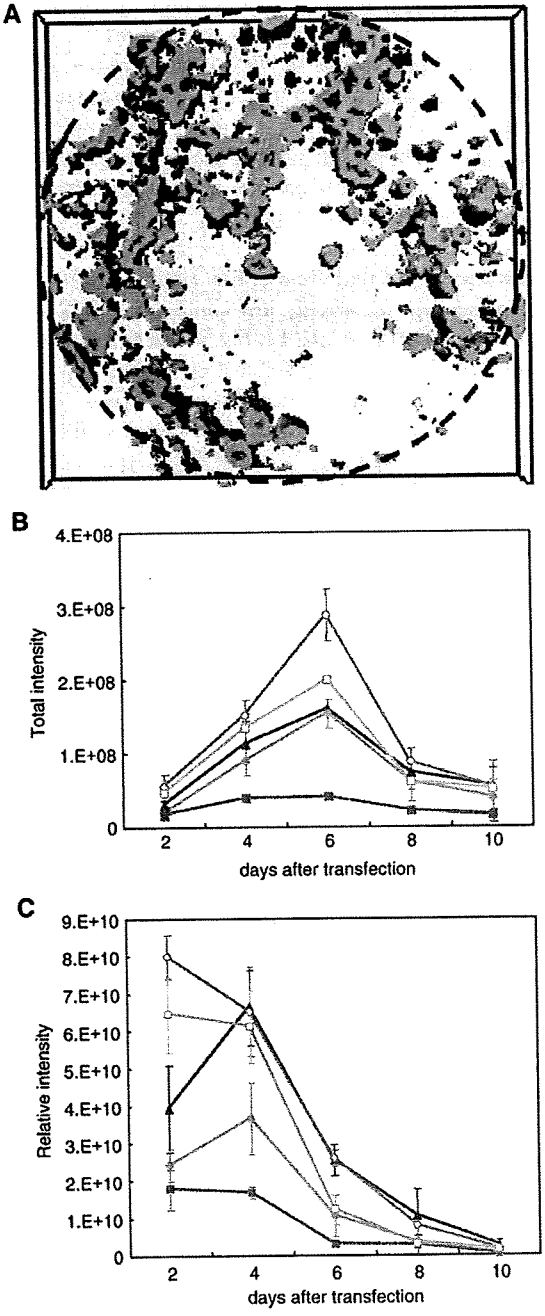

Fig. 6. Quantitative results of transfected fluorescent protein *Venus* in MCTS. A) Piled up images of transfected protein *Venus* from each slice by Imaris^{tm} (Carl Zeiss). B) Day-course of the change in total intensity by transfection with P[Asp(DET)] polyplexes (□; *N/P*=10, ○; *N/P*=20) and PEG-*b*-P[Asp(DET)] polyplex micelles (■; *N/P*=10, ●; *N/P*=20, ▲; *N/P*=40). C) Relative intensity (=total intensity/volume of spheroid) of fluorescence from transfected protein *Venus* with P[Asp(DET)] polyplexes (□; *N/P*=10, □; *N/P*=20) and PEG-*b*-P[Asp(DET)] polyplex micelles (■; *N/P*=10, ●; *N/P*=20, ▲; *N/P*=40).

3.6. DOPS-induced destabilization of P[Asp(DET)] polyplex and PEG-b-P[Asp(DET)] micelle

The differences in the time-dependency of the gene expression evaluated from the relative fluorescent intensity between P[Asp(DET)] polyplexes and PEG-*b*-P[Asp(DET)] micelles in Fig. 6C may reflect the differences in their behaviors after the internalization into the cell, because the transfection medium was replaced with fresh medium without polyplexes or micelles after 24 h. We therefore hypothesized that PEG-*b*-P[Asp(DET)] micelles may have greater stability or tolerability against pDNA unpacking, which is presumably induced through the exchange reaction with anionic components in the intracellular compartments, than P[Asp(DET)] polyplexes, thereby showing delayed gene expression. Thus, we evaluated the stability of the polyplex and polyplex micelle in the presence of anionic lipids (DOPS) as natural anionic compounds. It is known that such anionic lipids including phosphatidylserine exist appreciably in the intracellular compartments. As shown in Fig. 7, P[Asp(DET)] polyplexes (*N/P*=20) released pDNA at the [carboxyl groups in DOPS]/[phosphate groups in pDNA] (A/P) ratio of 12, whereas PEG-*b*-P[Asp(DET)] micelles (*N/P*=20) showed no pDNA release even at the highest *A/P* ratio (~ 17). Thus, PEG-*b*-P[Asp(DET)] micelles were judged to have higher tolerability against DOPS-induced destabilization than P[Asp(DET)] polyplexes.

4. Discussion

In this study, we prepared sets of cationic poly(*N*-substituted asparagine) homopolymers and PEG-*b*-poly(*N*-substituted asparagine) copolymers having the *N*-(2-aminoethyl)-2-aminoethyl group (P[Asp(DET)]) or *N*-(3-aminopropyl)-3-aminopropyl group (P[Asp(DPT)]) in the side chain (Scheme 1) to form polyplex-type non-viral gene vectors. To study the effects of the chemical structures of polycations and the effects of PEGylation of polycations on the properties as non-viral vectors, we carried out gene transfection to HuH-7 cells in the forms of monolayer culture and MCTS.

The in vitro evaluation of non-viral gene vectors relies mostly on the transfection study against monolayer cultured cells. However, there appear to be significant discrepancies between the environments of monolayer culture and in vivo tissues. One of these discrepancies is the short observable terms of the conventional monolayer cultures, which might prevent the study of the time-dependent properties of the gene expression of non-viral vectors. Especially for the polymeric gene delivery systems (polyplexes), in which pDNA is substantially condensed by

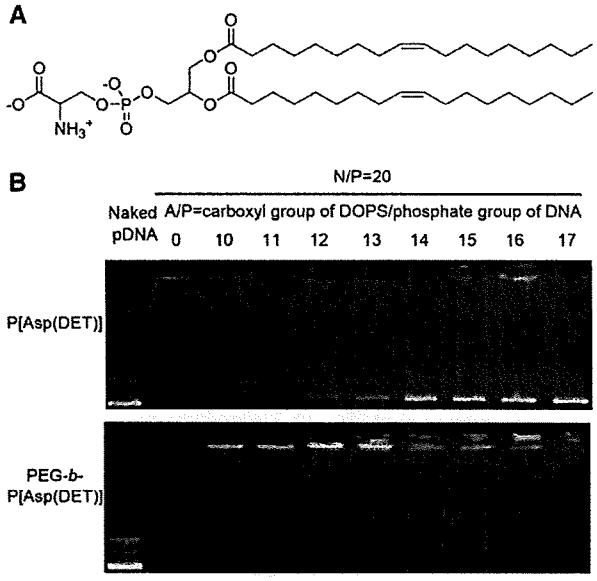

Fig. 7. Electrophoresis of P[Asp(DET)] polyplex and PEG-*b*-P[Asp(DET)] polyplex micelle. A) Chemical structure of anionic lipid (DOPS). B) Electrophoresis of P[Asp(DET)] polyplex and PEG-*b*-P[Asp(DET)] polyplex micelle solutions prepared at the *N/P* ratio of 20 after mixing with anionic lipid, DOPS at different *A/P* ratios.

cationic polymers and in some cases protected by biocompatible polymers to improve stability in biological media [9–12], prolonged evaluation of the gene expression might be necessary because it may take time for the decondensation and the release (the unpacking process) of pDNA from the polyplexes. Another important discrepancy between in vitro conventional monolayer cultures and in vivo tissues is the three-dimensional environments (e.g., cell–cell and cell–ECM interactions) for the cells. Thus, the three-dimensional features of in vivo tissues should be considered for in vitro evaluation of gene transfection. In this regard, three-dimensional multicellular spheroids (MCTS) might be a promising in vitro model for the evaluation of non-viral vectors worked under in vivo conditions.

In the transfection study using MCTS models, a long-term life span of MCTS might allow the prolonged evaluation of gene expression by non-viral vectors. Indeed, the spheroids transfected with the polyplexes showed the gene expression of fluorescent protein for over 10 days (Figs. 5 and 6). We also found that the small spheroids with diameters of ca 100 μm were more sensitive against the polyplex-induced cytotoxicity than monolayer cultured cells, while relatively large (ca 700 nm) MCTS did not show such high sensitivity to polyplex-induced toxicity (data not shown). It appears that the small spheroids may have a relatively weak structure due to their immature development of cell–cell and cell–ECM interactions. In contrast, the large spheroids have a heterogeneous structure consisting of outer layers of viable cells and a solid core of necrotic or hypoxic cells (Fig. 4C), resembling a monolayer cell culture where the cells adhere to the hard substrate. Such morphological differences between small and large spheroids may account for their different sensitivities against polyplex-induced cytotoxicity.

Among the evaluated polyplexes from the cationic homopolymers, P[Asp(DET)] polyplexes showed the most efficient transfection efficiency with the least cytotoxicity against monolayer cultured cells (Figs. 2 and 3). The efficient transfection by P[Asp (DET)] may be explained by their buffering capacity (Fig. 1A), which may facilitate the cytoplasmic delivery of the polyplexes through destabilization of the endosomal membrane by an increased ion osmotic pressure (proton sponge effect) [2]. However, P[Asp(DPT)] polyplexes at $N/P=10$ also showed an appreciably high transfection activity (Fig. 2A) regardless of the lack of proton buffering capacity (Fig. 1A), suggesting that the proton sponge effect may not fully explain the efficient gene transfection by P[Asp (DPT)] polyplex. Detailed mechanisms involved in the gene transfection process of P[Asp(DET)] and P[Asp(DPT)] polyplexes are under investigation in our laboratory and will be reported elsewhere in the near future. The cytotoxicity of P[Asp(DET)] polyplexes was remarkably low compared with other polyplexes from P[Asp(DPT)] or L/BPEI (Fig. 3). Also, the transfection study using MCTS models revealed that P[Asp(DET)] polyplexes at $N/P=10$ and 20 showed successful transfection with maintaining the MCTS structures, while the destruction of MCTS occurred by challenging L/BPEI and P[Asp(DPT)] polyplexes (Fig. 5B). The destruction of MCTS by the polyplexes (Fig. 5B) is in line with the cytotoxicity of the polyplexes against the monolayer cultured cells (Fig. 3), indicating the minimally cytotoxic nature of P[Asp(DET)] polyplexes. The unique molecular feature of a franking ethylenediamine unit, including a specific *gauche*-conformation of the mono-protonated form preferential at the physiological state, may have a role in this appreciably high biocompatibility of P[Asp (DET)] polyplexes. This hypothesis remains to be clarified yet.

PEGylation of polycations apparently improved the biocompatibility of polyplexes, as indicated by the stability of the MCTS structure after transfection. The PEG-*b*-P[Asp(DPT)] polyplex micelles at $N/P=10$ did not cause the destruction of the MCTS (Fig. 5C), whereas the destruction occurred through the transfection with P[Asp(DPT)] polyplexes at the same *N/P* ratio (Fig. 5B). Likewise, the PEG-*b*-P[Asp(DET)] polyplex micelles at $N/P=40$ showed no MCTS destruction, while the destruction of MCTS was observed in the transfection with the P[Asp(DET)] polyplexes at the same *N/P* ratio. Note that such a difference in biocompatibility between PEG-*b*-P[Asp(DET)] polyplex micelles and P[Asp(DET)] polyplexes could not be detected by the cytotoxicity study using the monolayer cultured cells, but was detected using the MCTS models. This result suggests that MCTS models are more sensitive than monolayer cultured cells to polyplex-induced toxicity, allowing them to detect the improved biocompatibility of the polyplex system through the PEGylation of polycations. Besides its positive effect of improving the cytotoxicity of the polyplexes, PEGylation of the polyplex changed the time-dependent profiles of the transfected gene expression. As seen in Fig. 6C, the relative intensity of the transfected fluorescent protein (i.e., *Venus*) in MCTS, which is defined as the total intensity divided by the volume of spheroids, followed significantly different time courses between P[Asp(DET)] polyplexes and PEG-*b*-P[Asp(DET)] polyplex micelles: the latter with relatively high *N/P* ratios, such as 20 and 40, had peak relative intensities at 4 days after transfection, while the former exhibited a continuous decrease in the relative

intensities with time (Fig. 6C). These results suggest that the polyplex micelles from PEG-*b*-polycation copolymers may be capable of delaying gene expression compared with polyplexes from cationic homopolymers. This is consistent with our previous report that in vivo gene expression of polyplex micelles in the liver revealed a delayed onset, and was observed 5 days after intravenous injection [13]. We hypothesized that such delayed gene expression from the polyplex micelles might be due to their higher stability or their delayed unpacking of pDNA in intracellular compartments. This may be supported from the increased tolerability of PEG-*b*-P[Asp(DET)] polyplex micelles compared to P[Asp(DET)] polyplexes against the pDNA exchange reaction with an anionic lipid, DOPS (Fig. 7). It is also consistent with our previous report that PEG-*b*-poly(L-lysine) polyplex micelles showed higher stability than poly(L-lysine) polyplexes in the thermal melting study of DNA [8]. The decrease in the local permittivity of the polyplex core, surrounded by PEG palisades and/or a steric protection of the polyplex core by PEG palisades, may contribute to the stabilization of polyplex micelles against the exchange reaction with anionic components in intracellular environments. It is worth noting that the time-dependency of gene expression differs between polyplex systems, which was clearly investigated through the prolonged observation of transfected cells in the form of spheroids.

In conclusion, we used MCTS models to study the effects of chemical structures and PEGylation of cationic poly(*N*-substituted asparagine) polyplexes on gene transfection, particularly focusing on both polyplex toxicity and the duration of gene expression. Through this evaluation, the feasible properties, i.e., biocompatibility and prolonged gene expression, of PEG-*b*-P[Asp(DET)] micelles were clarified, facilitating their utility for in vivo gene transfection as recently demonstrated in a rabbit carotid artery model [15]. Also, this study underscores the usefulness of MCTS models in screening non-viral vectors in conditions mimicking in vivo environments.

Acknowledgement

We are grateful to Mr. S. Fukushima and Mr. S. Asano for polymer synthesis. This work was supported by the Core Research for Evolutional Science and Technology (CREST), Japan Science and Technology Agency (JST), and the Health and Labor Sciences Research Grants in Research on Advanced Medical Technology in Nanomedicine Area from the Ministry of Health, Labor and Welfare (MHLW), Japan.

Appendix A. Supplementary data

Supplementary data associated with this article can be found, in the online version, at doi:10.1016/j.jconrel.2007.05.012.

References

[1] G.Y. Wu, C.H. Wu, Receptor-mediated in vitro gene transformation by a soluble DNA carrier system, J. Biol. Chem. 262 (1987) 4429–4432.
[2] O. Boussif, F. Lezoualc'h, M.A. Zanta, M.D. Mergny, D. Scherman, B. Demeneix, J.P. Behr, A versatile vector for gene and oligonucleotide transfer into cells in culture and in vivo: Polyethyleneimine, Proc. Natl. Acad. Sci. U. S. A. 92 (1995) 7297–7301.
[3] D.W. Pack, A. Hoffman, S. Pun, P.S. Stayton, Design and development of polymers for gene delivery, Nat. Rev. Drug. Discov. 4 (2005) 581–593.
[4] A.V. Kabanov, I.V. Astafieva, I.V. Maksimova, E.M. Lukanidin, G.P. Georgiev, V.A. Kabanov, Efficient transformation of mammalian cells using DNA interpolyelectrolyte complexes with carbon chain polycations, Bioconjug. Chem. 4 (1993) 448–454.
[5] M. Harada-Shiba, K. Yamauchi, A. Harada, I. Takamisawa, K. Shimokado, K. Kataoka, Polyion complex micelles as vectors in gene therapy — pharmacokinetics and in vivo gene transfer, Gene Ther. 9 (2002) 407–414.
[6] M. Ogris, E. Wagner, Targeting tumors with non-viral gene delivery systems, Drug Discov. Today 7 (2002) 479–485.
[7] K. Kataoka, G.S. Kwon, M. Yokoyama, T. Okano, Y. Sakurai, Block copolymer micelles as vehicles for drug delivery, J. Control. Release 24 (1993) 119–132.
[8] S. Katayose, K. Kataoka, Water-soluble polyion complex associates of DNA and poly(ethylene glycol)-poly(l-lysine) block copolymer, Bioconjug. Chem. 8 (1997) 702–707.
[9] M. Ogris, S. Brunner, S. Schüller, S. Kircheis, E. Wagner, PEGylated DNA/transferrin-PEI complexes: reduced interaction with blood components, extended circulation in blood and potential for systemic gene delivery, Gene Ther. 6 (1999) 595–605.
[10] T. Merdan, K. Kunath, H. Petersen, U. Bakowsky, K.H. Voigt, J. Kopecek, T. Kissel, PEGylation of poly(ethylene imine) affects stability of complexes with plasmid DNA under in vivo conditions in a dose-dependent manner after intravenous injection in to mice, Bioconjug. Chem. 16 (2005) 785–792.
[11] K. Itaka, A. Harada, K. Nakamura, H. Kawaguchi, K. Kataoka, Evaluation by fluorescence resonance energy transfer of the stability of nonviral gene delivery vectors under physiological conditions, Biomacromolecules 3 (2002) 841–845.
[12] K. Itaka, K. Yamauchi, A. Harada, K. Nakamura, H. Kawaguchi, K. Kataoka, Polyion complex micelles from plasmid DNA and poly(ethylene glycol)-poly (l-lysine) block copolymers as serum-tolerable polyplex system: physicochemical properties of micelles relevant to gene transfection efficiency, Biomaterials 24 (2003) 4495–4506.
[13] K. Miyata, Y. Kakizawa, N. Nishiyama, Y. Yamasaki, T. Watanabe, M. Kohara, K. Kataoka, Freeze-dried formulations for in vivo gene delivery of PEGylated polyplex micelles with disulfide crosslinked cores to the liver, J. Control. Release 109 (2005) 15–23.
[14] N. Kanayama, S. Fukushima, N. Nishiyama, K. Itaka, W.D. Jang, K. Miyata, Y. Yamasaki, U.I. Chung, K. Kataoka, A PEG-based biocompatible block catiomer with high buffering capacity for the construction of polyplex micelles showing efficient gene transfer toward primary cells, Chem. Med. Chem. 1 (2006) 439–444.
[15] D. Akagi, M. Oba, H. Koyama, N. Nishiyama, S. Fukushima, T. Miyata, H. Nagawa, K. Kataoka, Biocompatible micellar nanovectors achieve efficient gene transfer to vascular lesions without cytotoxicity and thrombus formation. Gene Therapy, in press.
[16] R.M. Sutherland, Cell and environment interactions in tumor microregions: the multicell spheroid model, Science 240 (1988) 177–184.
[17] H.R. Mellor, L.A. Davies, H. Caspar, C.R. Pringle, S.C. Hyde, D.R. Gill, R. Callaghan, Optimising non-viral gene delivery in a tumour spheroid model, J. Gene Med. 8 (2006) 1160–1170.
[18] H. Niwa, K. Yamamura, J. Miyazaki, Efficient selection for high-expression transfectants with a novel eukaryotic vector, Gene 108 (1991) 193–199.
[19] T. Nagai, K. Ibata, E.S. Park, M. Kubota, K. Mikoshiba, A. Miyawaki, A variant of yellow fluorescent protein with fast and efficient mutation for cell-biological application, Nat. Biotechnol. 20 (2002) 87–90.
[20] G.P. Tang, J.M. Zeng, S.J. Gao, Y.X. Ma, L. Shi, Y. Li, H.P. Too, S. Wang, Polyethylene glycol modified polyethylenimine for improved CNS gene transfer, Biomaterials 24 (2003) 2351–2362.
[21] M. Haji-Karim, J. Carlsson, Proliferation and viability in cellular spheroids of human origin, Cancer Res. 38 (1978) 1457–1464.
[22] L.A. Kunz-Schughart, Multicellular tumor spheroids; intermediates between monolayer culture and in vivo tumor, Cell Biol. Int. 23 (1999) 157–161.